Microwave Discharge of Nitrogen and Oxygen Gas Mixture for UV Light Source

Bimal Kumar Pramanik

A dissertation submitted to Kochi University of
Technology in partial fulfillment of the requirements
for the degree of Doctor of Philosophy

Department of Electronic and Photonic Systems Engineering
Kochi University of Technology
September- 2008

Abstract

This research focuses on the study of the emission spectrum from microwave discharge of N_2 /O_2 gas mixture in the UV and visible range (from 200 – 800 nm) in a cylindrical quartz tube aiming to apply it as a mercury free electrode less UV light source which can be used for water purification. N_2 /O_2 discharge emits intensive UV light in the 210 nm to 315 nm region which has germicidal effect. We investigated the dependence of gas composition and total pressure on the intensity of the UV emission. The experimental results showed that the UV intensity in 2100- 315 nm region varies with gas composition and pressure. In the examined condition, the highest was obtained at 20% O_2 concentration and 500 Pa total pressure.

In this research, experiments were carried out to study the effect of inert gases on the intensity of the emission from N_2 /O_2 discharge. He, Ne, Ar, Kr and Xe gases were used at different percentages of concentration. It was observed that at low concentration below 5%, these gases have no effect on the emission intensity whereas the emission intensity in both the UV and visible ranges decreased as the rare gas concentration was increased. The gases only behave as buffer gases. Buffer gases caused collisions with the other co-existing molecules and decreases the emission intensity.

Long time operation of microwave excited N_2 /O_2 gas mixture discharge without refreshing the enclosed gas was also conducted. To avoid degradation of enclosed molecular gases through chemical reactions with electrodes, we used electrode less microwave excitation for discharge in closed quartz discharge tubes. It was found that the intensity of NO peaks decreased with time due to the decrease of O_2

concentration inside the closed tube with operation time. Within 1 hour of operation, O_2 concentration decreased from 20% to 5% and in the following 10 hours, O_2 concentration reached to almost 1%. The pressure of N_2 also decreased with time. After several 10 hours of operation the pressure of N_2 dropped to a level which is not enough to sustain the plasma.

In this study, we also estimated UV, germicidal UV and effective germicidal power density in comparison with a low pressure commercial mercury lamp (GL10). The UV (200 -400 nm) power density was 1100 $\mu W/cm^2$ from N_2/O_2 discharge and was 180 $\mu W/cm^2$ from GL10 lamp. Power density in the germicidal range (210 nm t0 315 nm) was 470 $\mu W/cm^2$ from N_2/O_2 discharge and was 170 $\mu W/cm^2$ from GL10 lamp whereas the effective germicidal power density was 170 $\mu W/cm^2$ from N_2/O_2 discharge and was 120 $\mu W/cm^2$ from GL10 lamp. In case of Hg lamp, 95% of the UV light is emitted in the germicidal region and 65% of the total UV light is effective in germicidal action. On the other hand, in case of N_2/O_2 discharge 45% of the UV light is emitted in the germicidal range and only 15% of it is effective in germicidal action.

Acknowledgement

This research work was performed in the “Hatta Laboratory”, Department of Electronic and Photonic Systems Engineering, Kochi University of Technology during the years from 2005 to 2008.

First, I would like to express my deepest gratitude to my supervisor, Professor Akimitsu Hatta, for providing me the opportunity to work with his group for three years. In addition, I owe him my sincere appreciation for his guidance and encouragement during this work. I would also like to thank him for supporting me to join several conferences to get more helpful information for writing this thesis.

The author is grateful to Prof. Jinno and Dr. Motomura of Ehime University who has provided me with the closed quartz tube filled with N_2/O_2 gas mixture for my experiments and given several fruitful comments and suggestions for this study.

I wish to extend my sincere thanks to Prof. Hiroshi Kanbe, Prof. Masahiro Kimura, Prof. Katsushi Iwashita and Prof. Tadashi Narusawa, members of evaluation committee, for their useful comments and suggestions for the improvement of the study.

I want to thank all my colleagues working at the “Hatta Laboratory” for the innovative and pleasant working environment. Especially I am grateful to Mr. Keishi Yanai and Mr. Kazumasa Kawamura for their kind help during my experiments. I am most grateful to Dr. Jun Seok Oh for his encouragement, friendship, and for the numerous discussions.

Finally, my sincerely thanks belong to my dear wife, for all of love, patience, and encouragement. Thank you for standing by me during both good and bad times.

Table of Contents

List of Figures

List of Tables

Chapter 1

Introduction

Energetic UV radiations have found many technical applications in various biological, physical and chemical processes. Examples include disinfection of drinking water [1-8], sterilization of medical equipments [4-8], photochemical synthesis [9], and photo-enhanced chemical vapor deposition [10-11]. Recently UV irradiation of water has been established as a mature alternative to chlorination for disinfection of drinking water [12] . However Hg which is used today as filling element in the UV light source is highly toxic. Environmental groups worldwide are calling for limits on the use of mercury in electrical and electronic equipment. So the replacement of mercury in conventional UV lamps by other components is highly desirable.

Ultraviolet (UV) light is electromagnetic radiation with a wavelength shorter than that of visible light, but longer than X-rays. The range of electromagnetic radiation is shown in figure 1.1. Ultraviolet light is not visible to the human eye. UV light is typically found as part of the radiation received by the Earth from the Sun. The Sun emits ultraviolet radiation in the UVA, UVB, and UVC bands, but because of absorption in the atmosphere's ozone layer, 98.7% of the ultraviolet radiation that reaches the Earth's surface is UVA. The UV spectrum has many effects, including both beneficial and damaging changes to human health. In 1801 the German physicist Johann Wilhelm Ritter made the hallmark observation that invisible rays just beyond

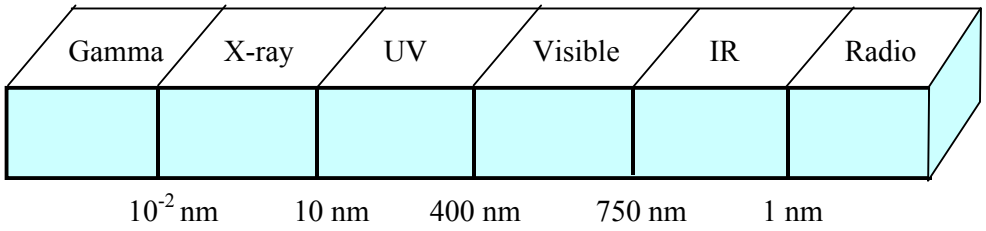

Fig. 1.1: Range of electromagnetic waves

the violet end of the visible spectrum were responsible for darkening silver salts when exposed to sunlight [1]. He called them "de-oxidizing rays" to emphasize their chemical

Table 1.1: Wavelength range of the various subdivisions of UV light

Type	**Wavelength range**
Ultraviolet A (UVA)	400 nm – 315 nm
Near UV (NUV)	400 nm – 300 nm
Ultraviolet B or Medium wave (UVB)	315 nm – 280 nm
Middle UV (MUV)	300 nm – 200 nm
Ultraviolet A, short wavr or germicidal (UVC)	280 nm – 100 nm
Far UV (FUV)	200 nm – 122 nm
Vacuum UV (VUV)	200 nm – 10 nm
Extreme UV (EUV)	121 nm – 10 nm

reactivity. The simpler term "chemical rays" was adopted shortly thereafter, and it remained popular throughout the 19th century. The term chemical ray was eventually dropped in favor of ultraviolet radiation [2]. The electromagnetic spectrum of ultraviolet light can be subdivided in a number of ways. The draft ISO standard on determining solar irradiances (ISO-DIS-21348)[13] describes the following ranges as shown in table 1.1.

1.1 Applications of UV

UV radiations have many applications in different fields. Some of the important applications are mentioned here:

1.1.1 Sterilization

UV light is used to sterilize workplaces and biological and medical tools used in laboratories and medical facilities [3-7]. Commercially-available low pressure Hg lamp that emits light at 254 nm is widely used for this purpose. The light emitted at 254 nm has the highest the germicidal effect on the germicidal effectiveness curve (i.e., effectiveness for UV absorption by DNA)[1].

1.1.2 Disinfection of drinking water

UV radiation can be an effectively used to kill virus and bacteria. UV radiation is used for disinfection of drinking water and pool water [8]. Recently UV irradiation of water has been established as a mature alternative to chlorination for disinfection of drinking water [9] . Many companies use UV disinfection equipment to sterilize spring water before bottling. New York City has approved the construction of a 2 billion gallon per day ultraviolet drinking water disinfection facility [14]. A process named SODIS [2]

has been intensively researched in Switzerland and has proven ideal to treat small quantities of water using natural sunlight.

1.1.3 Spectrophotometry

For analyzing chemical structure of materials, UV/VIS spectroscopy is widely used as a powerful technique in chemistry. UV radiation is often used in visible spectrophotometry to determine the existence of fluorescence in a given sample.

1.1.4 Photolithography

Photolithography is extensively used in the electronics industry for manufacturing semiconductor devices and integrated circuit components [15-17]. Photolithography is a process used to transfer circuit patterns onto a semiconductor wafer.Ultraviolet radiation is used for very fine resolution photolithography.

1.1.5 Analyzing minerals

Ultraviolet light is also used in analyzing minerals, gems, and in other detective work. Under visible light different materials may look the same, but under ultraviolet light they fluoresce to different degrees.

1.1.6 Astronomy

Ultraviolet astronomy uses ultraviolet wavelengths between approximately 100 and 3200 E (10 to 320 nm)[18] which is best suited to the study of thermal radiation and spectral emission lines from hot blue stars that are very bright in this wave band. Most UV observations are made from space as the ozone layer blocks many UV frequencies

from reaching telescopes on the surface of the Earth.

1.1.7 Security purpose

To ensure the security of sensitive documents (e.g. credit cards, driver's licenses, passports) many countries include a UV watermark/ stickers on them that are invisible to the naked eye under normal lights, but strongly visible under UV illumination. Banknotes of various countries have an image, as well as many multicolored fibers, that are visible only under ultraviolet light.

1.1.8 Pest control

Ultraviolet traps are used to eliminate various small flying insects. They are attracted to the UV light, and are killed using an electric shock, or trapped once they come into contact with the device. Different designs of ultraviolet light traps are also used by entomologists for collecting nocturnal insects during faunistic survey studies.

1.1.9 Chemical markers

UV fluorescent dyes are used in many applications (for example, biochemistry and forensics). Many substances, such as proteins, have significant light absorption bands in the ultraviolet that are of use and interest in biochemistry and related fields.

1.1.10 Checking of electric insulation

Detection of corona discharge (often simply called "corona") on electrical apparatuses is a new application of UV light. Degradation of insulation of electrical apparatus or pollution causes corona causing the emission of ultraviolet radiation.

1.1.11 Food processing

As the demand for fresh and safe food products increases, the demand for nonthermal and improved food processing methods is also increasing. Ultraviolet radiation is used in several food processes to remove unwanted microorganism. UV light can be used to pasteurize fruit juices by flowing the juice over a high intensity ultraviolet light source.

1.1.12 Curing of inks, adhesives, varnishes and coatings

UV light is used for polymerization of organic coatings and paints [19-20]. Certain inks, coatings and adhesives when exposed to the correct energy and irradiance in the required band of UV light, polymerization occurs, and so the adhesives harden or cure. Many industries have developed UV lamps for UV curing applictions.

1.1.13 Photo-enhanced chemical vapor deposition

UV light is also used in semiconductor industries for fabrication. UV light is used in Photo-enhanced chemical vapour deposition for fabrication of certain materials [21-22] .

1.2 Disinfection of water by UV light

Bactericidal effect of radiant energy from sunlight was first reported in 1877 [23]. The technical use of UV light made progress after the discovery of the mercury vapor lamp by Hewitt in 1901 and the first disinfection of drinking water was done at the city of Marseille in France in 1910. The method of inactivation of water-endurable microorganisms and viruses by means of UV irradiation has proved its effectiveness.

This method does not spoil taste and smell of water after treatment and does not bring any undesirable by-products in water. It is rapidly gaining in popularity as the alternative to conventional reagent techniques.

1.2.1 Mechanism of disinfection

The disinfection of microorganisms with UV light is fundamentally a photochemical process. So the effectiveness of disinfection by this process depends on the amount of UV light absorbed by the microorganisms. The absorption by cellular material results from absorption by protein and by nucleic acids (DNA and RNA). UV irradiation photochemically damages or alters the DNA of the microorganisms. Decay of microorganism occurs due to the lack of capability of further multiplication of the microorganism with damaged nucleic acids. UV light at different wavelengths is not equally absorbed by the nucleic acids of the microorganisms. As for example, UV light emitted at 254 nm is mostly absorbed while only small portion of UV light at 290 nm is absorbed. So the effective germicidal efficiency of UV light at different wavelengths is not equal. The effective germicidal efficiency of UV light varies with the wavelength of the emitted light having the maximum at 260 nm. The potential disinfection efficiency of UV light is presented in figure 1.2.

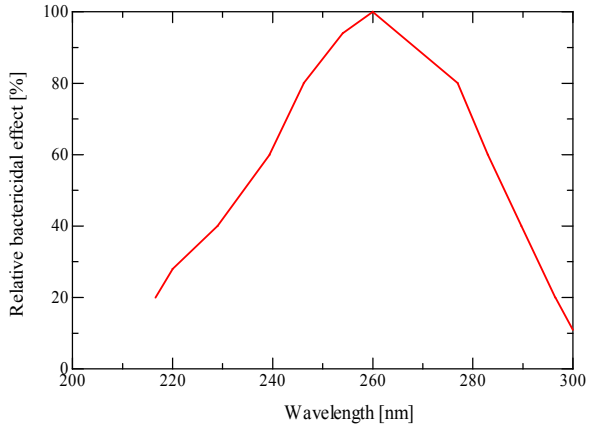

Fig.1.2: Germicidal efficiency distribution curve of UV light [1]

1.2.2 Dose of irradiation:

Irradiation dose is the total amount of energy that is transferred to water in the form of UV radiation. It is most commonly expressed as D_{10} value which represents the dose required to reduce the population by 90% [24].

The irradiation dose depends on three factors, namely:

i) Mean intensity of irradiation applied to water under treatment

ii) Time of its exposure to UV radiation and

iii) Water transparent index (T_{10}).

T_{10} is the percent of UV radiation remaining after its passing through a water layer of 10 mm in thickness. The lower T_{10} value, the larger the amount of energy required for disinfection. T_{10} value depends on the quality and on the potential elements present in the water. The dose of irradiation is measured in J/cm^2 or J/m^2 and is calculated by the formula:

$$D = I \times t$$

where I is the UV radiation density in W/cm^2 or W/m^2 and t is the time of exposure in second.

1.3 Overview of gas discharge plasmas

Plasmas are often called a fourth state of matter. A plasma is free charged particles moving in random directions that is, on the average, electrically neutral [25]. Plasma consists of positive ions, electrons as well as neutral species. The schematic view of plasma is shown in figure 1.3. It has been often said that 99% of the matter in the universe is in the plasma state [26]. This is certainly a reasonable one in view of the fact that stellar interiors and atmospheres, gaseous nebulae and much of the interstellar hydrogen are plasmas. Besides the astro-plasmas, we can classify the laboratory plasma in to two main groups, i.e. high temperature plasmas, and the low-temperature plasmas or gas discharges. Depending on the pressure in the plasma, the gas discharge plasmas can also be divided into 'local thermal equilibrium' (LTE) and non-LTE plasmas [27]. Indeed, a high gas pressure implies many collisions in the plasma (i.e. a short collision mean free path, compared to the discharge length), leading to an efficient energy exchange between the plasma species, and hence, equal temperatures. LTE discharges, which are characterized by rather high temperatures, are typically used for applications where heat is required, such as for cutting, spraying, welding or, as in the analytical ICP, for the evaporation of an analyte material. A low gas pressure, on the other hand, results in only a few collisions in the plasma (i.e. a long collision mean free path compared to the discharge length), and consequently, different temperatures of the plasma species due to inefficient energy transfer. Non-LTE plasmas, on the other hand, are typically used for applications where heat is not desirable, such as

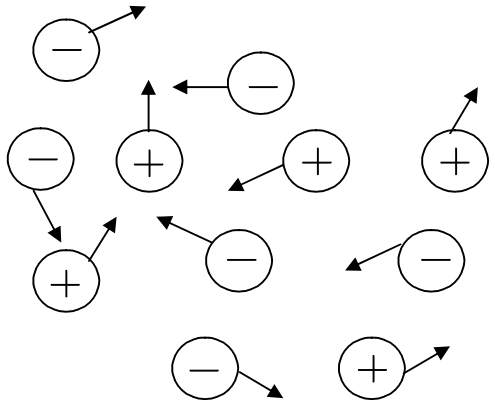

Fig. 1.3: Schematic view of plasma

for etching or the deposition of thin layers. In recent years, the field of gas discharge plasma applications has rapidly expanded. Because of multi-dimensional parameter of the plasma conditions, there exists a large variety of gas discharge plasmas, employed in a large range of applications. The important gas discharges are:

i) DC discharge

ii) Microwave discharge

iii) Capacitively coupled rf discharge

iv) Dielectric barrier discharges (DBDs)

v) Inductively coupled plasmas (ICPs)

In the following, an overview of two most important kinds of gas discharge plasmas will be presented.

1.3.1 DC discharge

The DC discharge is one of the most well studied gas discharges and widely applied to the plasma devices. In the simplest case, it is formed by applying a potential

difference (of a few 100 V to a few kV) between two electrodes that are inserted in a cell (or that form the walls of the cell). The cell is filled with a gas (an inert gas or a reactive gas) at a pressure ranging from a few mTorr to atmospheric pressure. When a sufficiently high potential difference is applied between two electrodes placed in a gas, the latter will break down into positive ions and electrons, giving rise to a gas discharge. The mechanism of the gas breakdown can be explained as follows: a few electrons are emitted from the electrodes due to the omnipresent cosmic radiation. Without applying a potential difference, the electrons emitted from the cathode are not able to sustain the discharge. However, when a potential difference is applied, the electrons are accelerated by the electric field in front of the cathode and collide with the gas atoms. The most important collisions are the inelastic collisions, leading to excitation and ionization. The excitation collisions, followed by de-excitations with the emission of radiation, are responsible for the characteristic name of the 'glow' discharge. The discharge can operate in a rare gas (most often argon or helium) or in a reactive gas (N_2, O_2, H_2, CH_4, Si H_4, SiF_4, etc.), as well as in a mixture of these gases [25].

Glow discharges are used in a large number of application fields. The most important application is probably in the microelectronics industry and in materials technology, for surface treatment, etching of surfaces (e.g., for the fabrication of integrated circuits), deposition of thin protective coatings, plasma polymerisation, plasma modification of polymers and other surfaces. This is also used in the light industry (e.g., fluorescence lamps, neon advertisements), as gas lasers, and as flat plasma display panels for the new generation of flat large area television screens.

1.3.2 Microwave discharge

MW can provide high power density with compared to other power sources and hence can produce high density plasma. In conventional dc discharges, the presence of the electrical connections and electrodes through the fused glass gives a limitation on the lifetime the plasma source. Microwave energy easily passes through the dielectric tube and so, unlike conventional lamps, they do not require electrodes [28]. All plasmas that are created by the injection of microwave power, i.e. electromagnetic radiation in the frequency range of 300 MHz to 10 GHz, can in principle be called 'microwave induced plasmas' (MIPs) [29-30]. This is, however, a general term which includes several different plasma types, e.g. cavity induced plasmas, free expanding atmospheric plasma torches, ECRs, surface wave discharges (SWD), etc. These different plasma types can operate over a wide range of conditions, i.e. a pressure ranging from less than 0.1 Pa to a few atmospheres, a power between a few W and several hundreds of kW. They can also sustain in both noble gases and molecular gases [29].

1.4 Motivation and aim of the work

UV radiations have many applications in biological, physical and chemical and other fields. The method of purification of drinking water by means of UV irradiation is rapidly gaining popularity as the alternative to conventional reagent techniques. Exposure of microbiological systems to UV light within the germicidal region from 210 to 315 nm results in the inactivation of the microorganisms. Irradiation with UV light of a wavelength of 254 nm kills or renders bacteria incapable of reproduction by photochemically altering the DNA in the cell[28]. S. Iseki et al. developed plasma sterilization system using atmospheric pressure plasma. They

reported that *Penicillium digitatum* was successfully sterilized using atmospheric pressure plasma [31]. Y. Ohtsu et al. investigated the inactivation of *Bacillus subtilis* spores using DBD plasma. They observed that the bacteria subtilis with 10^6 CFU/ml was sterilized within 20 min using He/ O_2 gas mixture and 60 W RF power [32]. H. Eto et al. carried out sterilization experiment of *Geobacillus stearothermophilus* spores using DBD under air circumstance and pure N_2 gas in atmospheric pressure [4]. They found that synergetic effect of ozone, UV and OH radicals affected sterilization event. N. Hayashi et al. examined the removal of protein from the surface of medical quipments using O_2 plasma produced by RF plasma. They were able to remove the protein from th surface of the equipments within several hours avoiding any damage to the equipments [33]. M. K. Singh et al. investigated low pressure plasma sterilization of *Geobacillus stearothermophilus* spores using MW plasma [5]. They reported that UV emission along with reactive species in the plasma was the main sterilizing factor. S. Kitazaki et al. examined the sterilization of the inner surface of a tube using an AC HV glow discharge at low pressure [6]. They found that a tube with length of 500mm and diameter 4 mm was successfully sterilized within 10 min using oxygen plasma. Kenji Ban et al. investigated the sterilization performance of microwave plasma using N_2/O_2/He gas mixture and they observed a better performance [34]. UV light is also used for purification of drinking water. Now-a-days UV irradiation of water has been established as a mature alternative to chlorination for disinfection of drinking water. A I Al- Shamma et al. developed a low power microwave plasma high intensity UV light. They reported that the lamp can be used for water purification and ozone applications [28].

Mercury which is used today as filling element in the UV light source is highly

toxic and potentially carcinogenic. These dangers, even in very small quantities, can eventually lead to neurological system and brain damage in humans. Along with other harmful elements, such as lead, cadmium, and hexavalent chromium, environmental groups worldwide are calling for limits on the use of mercury in electrical and electronic equipment. European Union's RoHS (Restriction of Hazardous Substances) has already banned the use of lead, mercury, cadmium, chromium, polybrominated biphenyls and polybrominated diphenyl ethers from electronics sold in EU member states beginning from 1 July 2006. So the replacement of mercury in conventional UV lamps by other components is highly desirable for environmental reasons. So now it is high time to find out the alternative of mercury as a light source. As reported by Hilbig et al. at LS-10 [35], molecular radiators are also options as mercury free light source. Research on molecular radiators is becoming popular with time. C. Fozza et al. investigated theVUV to near infrared emissions from molecular gas–noble gas mixtures (H_2–Ar and O_2–Ar) in order to obtain very intense VUV emissions from mixtures of gases, which can be useful for the photochemical treatment of polymer surfaces [36]. D Uhrlandt et al. demonstrated a mercury free plasma light source operating at low pressure below 1 kPa. In the experiment, rare gas mixture was used for discharge as a effort to study the possibility of replacing conventional mercury-containing lamps by plasma light source [37]. A. Kono et al. observed VUV emission from Ar and Xe using microwave excitation aiming to apply it as VUV excimer light source [38]. A. Rahman et al. measured the optical emission spectra in the 110–400 nm regions from radio-frequency-driven (13.56 MHz) hollow slot microplasmas operating in open air at atmospheric pressure and they compared the magnitude of light emission from the open air micro plasmas with values available from commercial UV mercury lamp [39].

The electrode less discharge lamps operated by MW power has been expected as next generation lamps since they are considered to achieve excellent properties such as long-life, high efficiency and gas components filled in the lamps are environmentally friendly. The presence of the electrical connections and electrodes through the fused glass gives a limitation on the lifetime of the source. In conventional gas discharge, the electrode also absorbs gas inside the tube and causes chemical reaction with them. Microwave energy easily passes through the dielectric tube and so, unlike conventional lamps, they do not require electrodes which are not only a weakness for the longevity of conventional lamps but, most importantly, limit the amount of power per unit length that the lamp can produce. Filling gases in the tube avoid the problems of chemical reactivity with electrode to a large extent. Therefore, they have attracted an increasing interest in the field of lamp industry. Recently, the novel high intensity discharge lamps such as sulfur lamp and cluster lamp [40] have been developed using MW power higher than 200 W. Masaya Shido et al. introduced long life and high efficiency electrode less mercury-free lamps for industrial application [29]. A low power MW of 2.45 GHz from a magnetron was applied for generating plasma. A I Al- Shamma et al. developed a UV light source driven by microwave power for water purification [25].

In this work, the emission spectrum from microwave discharge of N_2 /O_2 gas mixture in the UV and visible range (from 200 – 800 nm) was studied in a cylindrical quartz tube aiming to apply it as a mercury free electrode less UV light source which can be used for water purification. In conventional gas discharge, the electrode absorbs N_2 and O_2 gas and causes chemical reaction with them. In this research, the discharge is driven by microwave power and there is no electrodes and electrical connection through

the fused glass tube which increases life time of the source. As of N_2 /O_2 gas mixture contains no toxic element like mercury, it will not create any environmental problem.

1.5 Organization of the report

This report consists of 6 chapters. The organization of this report is shown in figure 1.4. It begins with chapter 1, which includes overview and applications of UV light. In addition, the overview of different kinds of gas discharge plasmas is discussed in this chapter. After that background and aim of the study are given.

In chapter 2, the production of microwave excited N_2/O_2 gas mixture discharge in a cylindrical quartz tube is described. The effect of gas composition and total gas pressure on the emission intensity is discussed in this chapter. Experimental method and the causes of variation of emission intensity with gas composition and gas pressure are also explained in details.

In chapters 3, the effect of inert gases on the emission intensity from microwave excited N_2 /O_2 gas mixture discharge is discussed. He, Ne, Ar, Kr and Xe gases at different percentages of concentration was used in the experiment. It was observed that at low concentration below 5%, these gases have no effect on the emission intensity whereas the emission intensity in both the UV and visible ranges decreased as the rare gas concentration was increased. The causes of the decrease of emission intensity in both the UV and visible range are also explained.

Long time operation of microwave excited N_2/O_2 gas mixture discharge

without refreshing the enclosed gas is discussed in chapter 4. The experimental method and the results obtained from the experiments are explained in the chapter.

In chapter 5, the measurement technique and the comparison of the of the intensity of the emitted radiation (in the UV and germicidal region) from the N_2/O_2 gas mixture microwave excited discharge and from low pressure commercial Hg lamp (MITSUBIHI/ OSRAM GL10) are discussed. In case of Hg lamp, 94% of the UV light is emitted in the germicidal region and 65% of the total UV light is effective in germicidal action. On the other hand, in case of N_2/O_2 discharge 45%, of the UV light is emitted in the germicidal range and only 15% of it is effective in germicidal action.

Finally, the summary of the study is given in chapter 6.

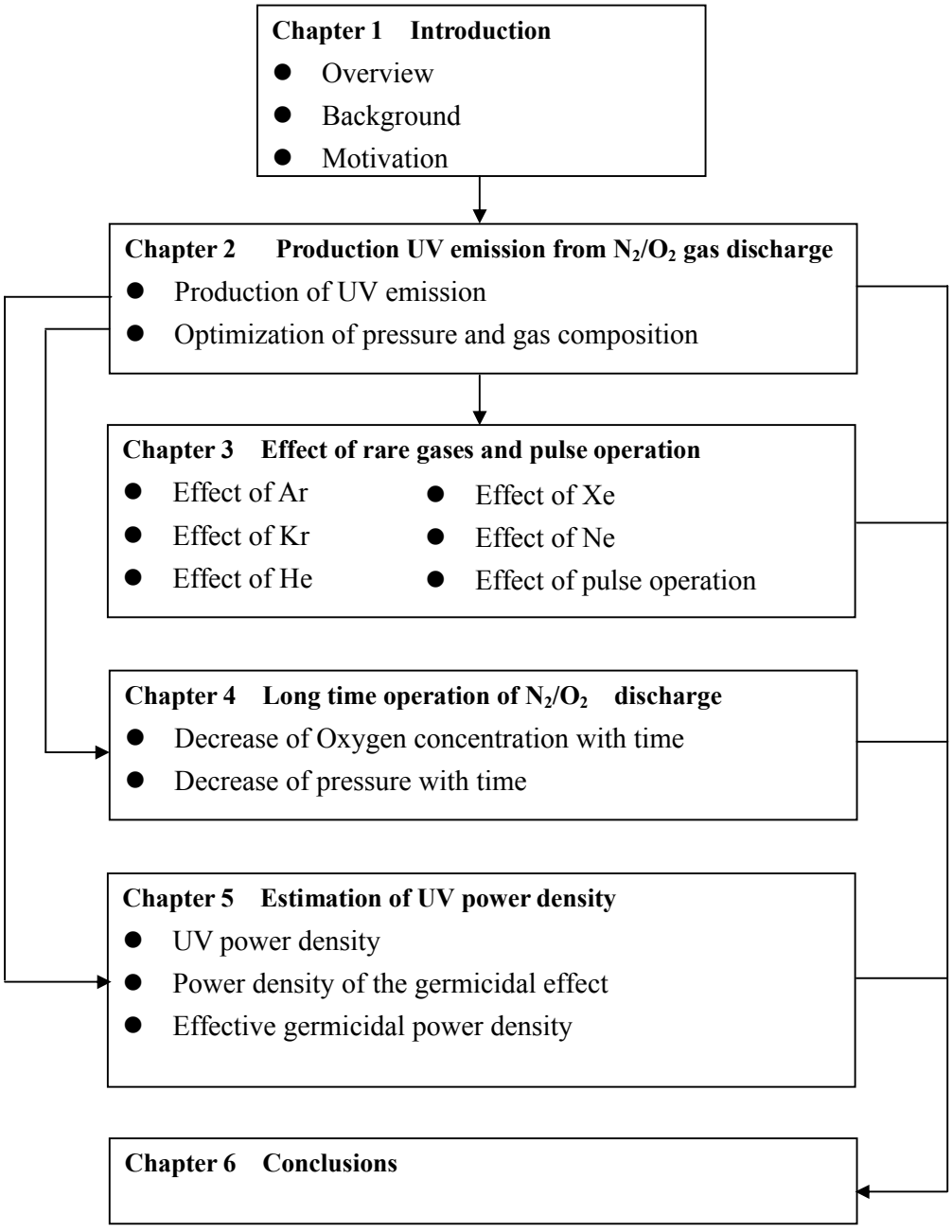

Fig. 1.4: Organization of the thesis

References:

[1] W. J. Massachelein, Ultraviolet light in Water and Wastewater Sanitation, Lewis publication (2002).

[2] P.E. Hockberger, Photochem. Photobiol., **76,** 561-579 (2002).

[3] Y. Ono, H. Eto, A. Ogino and M. Nagatsu, Proc. 25th Sym. on Plasma Processing, 119 (2008).

[4] H. Eto, Y. Ono, A. Ogino and M. Nagatsu, Proc. 25th Sym. on Plasma Processing, 125 (2008).

[5] M. K. Singh, S. Kojima, L. Xu, A. Ogino and M. Nagatsu, Proc. 25th Sym. on Plasma Processing, 229 (2008).

[6] S. Kitazaki and N. Hayashi, Proc. 25th Sym. on Plasma Processing, 243 (2008).

[7] M. Nagatsu, F. Terashita and Y. Koide, Jpn. J. Appl. Phys., **42,** 856-859 (2003).

[8] A. M. Braun, M. T. Maurette and E. Oliveros, Photochemical Technology, New York, Wiley (1991).

[9] O Legrini, E Oliveros and A M Braun, Chem. Rev., **93,** 671–98 (1993).

[10] J. Y. Zhang, H. Esrom and I. W. Boyd, Appl. Surf. Sci., **96,** 399–404 **(**1996).

[11] H. Esrom and U. Kogelschatz, Appl. Surf. Sci., **54,** 440–444 **(**1992).

[12] Z. Falkenstein, Development of an excimer UV light source system for water treatment, Ushio America, Inc. (2001).

[13] ISO 21348, Process for determining Solar Irradiance.

[14] D. Portoti, UV disinfection for New York city: Bridging design with operational strategis, American Water Works Association.

[15] M. Yashiaki, O. Takashi, T. Tatsuo and S. Kyozo, Jpn. J. Appl. Phys., **17**, 541-550

(1978).

[16]B. Torbiйro, M.L. Pourciel-Gouzy, I. Humenyuk, J.B. Doucet, A. Martinez and P. Temple-Boyer, Microelectronics Journal, **37**, 133-136 (2006).

[17] S. Kim, T. W. Kwon, J. Y. Kim, H. Shin and J. G. Lee, J. of the Korean Physical Society, **49**, 736-740 (2006).

[18] A. N. Cox, Allen`s astrophysical quantities, Springer-Verlag, New York, (2000).

[19] H. Boettcher, J. Bendig, M. A. Fox, G. Hopf and H. J. Timpe, Technical Applications of Photochemistry, Leipzig, Interdruck, (1991).

[20] R. S. Nohr and J. G. MacDonald, Radiat. Phys. Chem., **46,** 983–986 **(**1995).

[21] J. Y. Zhang, H. Esrom and I. W. Boyd, Appl. Surf. Sci., **96,** 399–404 **(**1996).

[22] H. Esrom and U. Kogelschatz, Appl. Surf. Sci., **54,** 440–444 **(**1992).

[23] A. Downes and T. P. Blunt, Proc. R. soc., **26**, 488 (1877).

[24] M. M. Garcia , Evaluation of gamma radiation levels for reducing pathogenic bacteria and Fungi in animal sewage and laboratory effluents, Can J Vet. Res., **51**, 285-289 (1987).

[25]. M.A. Lieberman, A.J. Lichtenberg, Principles of Plasma Discharges and Materials Processing, Wiley, New York, (1994).

[26] F. F. Chen, Introduction to plasma physics and controlled fusion, Plenum press, 2nd edition, New York and London.

[27] A. Bogaerts , Spectrochimica Acta, Part B, **57**, 609-658 (2002).

[28] A. I. Al-Shammaa, I. Pandidas and J. Lucas, J. Phys. D Appl. Phys., **34,** 2775-2781 (2001).

[29] E. Timermans, Atomic and molecular excitation processes in microwave induced plasma, Ph. D thesis, Eindhoven Uni. Of Techno. (1999).

[30] C. M. Ferreira and M. Moisan, Microwave discharges, Fundamentals and applications, NATO ASI series, Series B, **302**, Plenum, New York (1993).

[31] S. Iseki, Proc. 25 th Symo. on Plasma Processing, 55 (2008).

[32] Y. Ohtsu, Y. Miyazaki, T. Misawa and H. Fujita, Proc. 25th Sym. on Plasma Processing, 127 (2008).

[33] N. Hayashi and Y. Yagyu, Proc. 25th Sym. on Plasma Processing, 57 (2008).

[34] K. Ban, T. Ikeda and T. Aki, Proc. 22nd Sympo. on Plasma Processing, 114 (2005).

[35]. R. Hilbig, A. Koerber, J. Baier and R. Scholl, Proc. 10th int. Sym. on the Sci. and Techno. Of light sources, 75-84 (2004).

[36] A. C. Fozza, A. Kruse, A. Hollдnder, A. Ricard and M. R. Wertheimer. J. Vac. Sci. Techno. A: Vac. Surfaces, and Films, **16,** 72-77 (1998).

[37] D Uhrlandt, R Bissiahn, S Gorchakov, H Lange, D Loffgahen and D Notzold, J. Phys. D: Appl. Phys., **38,** 3318 (2005).

[38] A. Kono, J. Wang and M. Aramaki, Thin Solid Films, **506** 444-448 (2006).

[39] A. Rahman, A.P. Yalin, V. Surla, O. Stan, K. Hoshimiya, Z. Yu, Eric Littlefield and G.J. Collins, Plasma Sources Sci. and Techno., **13,** 537-547 (2004).

[40] Weber and R. Scholl, J. Appl. Phys. **74**, 607 (1993.

Chapter 2

Production of UV emission from N_2 /O_2 gas discharge

The physics of microwave discharges is a rapidly developing field of low-temperature physics [1]. Interest in this field is generated by promising applications of microwave discharges. The applications include plasma chemistry, gas lasers, light sources [2-3], disposal of toxic waste, development of artificial ionized clouds in the Earth atmosphere [1], ozone layer recovery, analytical chemistry, sensitive spectrometry [4], deposition of carbon materials [5-6] and others. The demand for microwave generated plasma is also increasing for many industrial applications as a high power source [7-12]. Microwave energy easily passes through the dielectric tube and so, unlike conventional lamps, they do not require electrodes which are a weakness for the longevity of conventional lamps. In conventional source, the electrode also absorbs gas and causes chemical reaction with them which decreases the life time of the source. So the demand for microwave plasma light source is increasing day-by-day for many applications. Al- Shamma et al. developed a low power microwave plasma Hg UV lamp for water purification and ozone applications [13]. Kono et al. produced VUV emission from Ar and Xe using microwave excitation aiming to apply it as VUV excimer light source [14]. Fozza et al. investigated the VUV to near infrared emissions from molecular gas–noble gas mixtures (H_2–Ar and O_2–Ar) to obtain very intense VUV emissions [15].

In this chapter, the emission spectrum from microwave gas discharge of N_2 /O_2 mixture in a cylindrical quartz tube in the UV and visible range (from 200 – 800 nm) is

described. The N_2 / O_2 mixture gas discharge emits intensive UV light in the 200 nm to 280 nm region which has germicidal effect. The dependence of gas composition on the intensity of UV emission is explained. The effect of pressure on the intensity of the UV emission is also discussed in this chapter. The experimental results showed that the UV intensity in 200- 280 nm region varied with gas composition and was highest at 20% O_2 concentration and 500 Pa.

2.1 Principle of emission of light

Light can be produced by activating electrons from lower orbital state (ground state) to a higher orbital state of an element. When this activated (excited) electron undergoes a transition from higher orbital state (excited state) to lower orbital state (ground state), it emits a photon. The process is schematically illustrated in figure 2.1. If an electron is in the excited state with energy E_2, it may sponteneously return to the ground state, with energy E_1, releasing the difference in energy between the two states as a photon. The photon will have frequency ν and energy hν: $E_2 - E_1 = h\nu$, where h is the plank's constant (6.626×10^{-34} J sec). This kind of emission is known as spontaneous emission which occurs in flames, or discharge lamps. Another kind of emission, stimulated emission occurs when matter in an excited state is perturbed by a photon of light and gives rise to a further photon of light, typically with the same energy and phase as the perturbing photon. This phenomenon is the process which gives rise to laser emission where you have many photons at the same wavelength and in phase with each other.

Thermal activation of matter also provides a means of production of light. A body at a given temperature emits a characteristic spectrum of light called black body

radiation. As for example, let us consider an electric filament as current is applied to it. As the electric current supplies energy to the filament and it heats up, it starts to glow red, and as it gets hotter it then turns orange and then white. The filament acts like a black body and as the filament gains energy from the electrical power it tries to equalize its energy with its surroundings by radiating its excess energy. It does this by emitting light starting first in the infrared and as the filament gets hotter or has more energy the radiation moves more into the visible spectrum. Black body radiation is not a main source for generation of UV light. At present, activation of mercury atoms by electrons (i.e., electrical discharge) is the most common technology for generating UV light used for water disinfection.

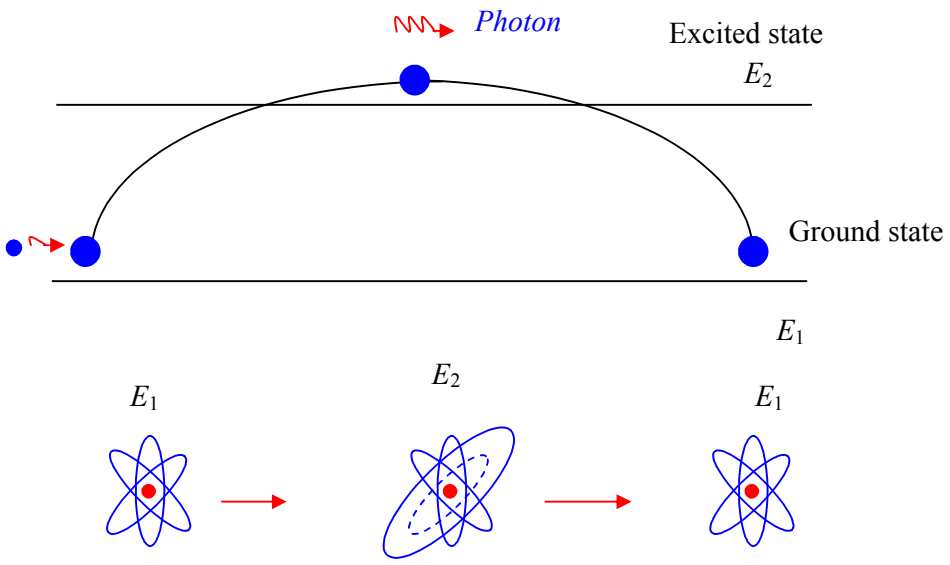

Fig.2.1: Schematic representation of emission of radiation by matter

2.2 Experimental apparatus

Brief description of the experimental apparatuses used in the experiments is given below.

2.2.1 Microwave generator and microwave applicator

The schematic view of microwave generator and microwave applicator is shown in figure 2.2. The microwave source used in the experiment was a magnetron power source operating at 2.45 GHz with power rating of up to 1.5 k W.

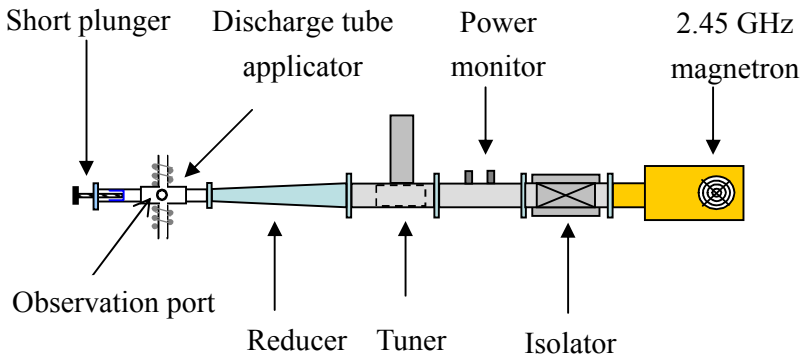

Fig. 2.2: Schematic diagram of microwave generator and microwave applicator

The isolator isolates the reflected power send it to a dummy load. Forward power and reflected power can be monitored through two power monitor ports. Power meters are connected to the monitor ports for the measurement of power. Separate meters are used to monitor forward and reflected power. The total applied power is the difference of the forward and reflected power. Tuner is used to minimize the reflected power. By adjusting the tuner position the amount of reflected power can be controlled. Reducer is

used to couple the microwave applicator to the microwave generator. As the dimension of the waveguide connected to the microwave generator and the dimension of the microwave applicator is not same, reducer is used.

A microwave applicator constructed from aluminum alloy was used in the experiment. The applicator has the dimension of 260 mm length, 100 mm width and 30 mm height. The power from the generator to the microwave applicator was fed through rectangular waveguide. The schematic view of the applicator is shown in figure 2.3.

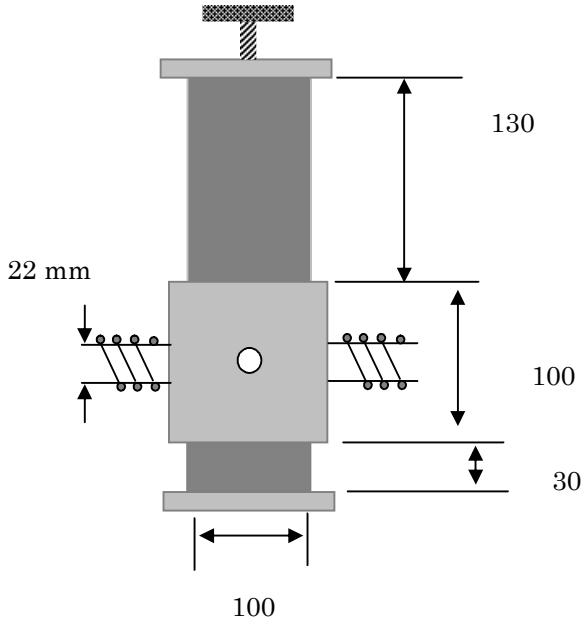

Fig.2.3: Microwave applicator used in the experiment

2.2.2 Spectrometers

A spectrometer is an optical instrument used to measure properties of light over a specific portion of the electromagnetic spectrum. The variable measured is most often the light's intensity. The independent variable is usually the wavelength of the light, normally expressed as some fraction of a meter, but sometimes expressed as some unit

directly proportional to the photon energy, such as wavenumber or electron volts, which has a reciprocal relationship to wavelength. A spectrometer is used in spectroscopy for producing spectral lines and measuring their wavelengths and intensities. The spectroscope was invented by both Gustav Robert Georg Kirchhoff and Robert Wilhelm Bunsen. In the original spectroscope design in the early 19th century, light entered a slit and a collimating lens transformed the light into a thin beam of parallel rays. The light was then passed through a prism (in hand-held spectroscopes, usually an Amici prism) that refracted the beam into a spectrum because different wavelengths were refracted different amounts due to dispersion. This image was then viewed through a tube with a scale that was transposed upon the spectral image, enabling its direct measurement. Modern spectrometers, generally use a diffraction grating, a movable slit, and some kind of photodetector, all automated and controlled by a computer. The schematic diagram of a Grating spectrometer is shown in figure 2.4. Two types of spectrometer, USB4000 and HR4000 were used in experiments. USB4000 was used for measuring the spectrum in the visible region whereas HR4000 was used to measure the spectrum in the UV range.

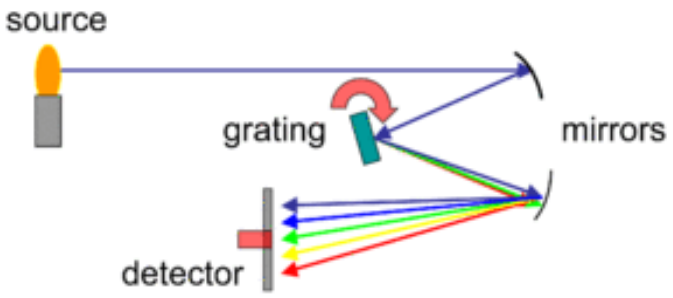

Fig.2.4: Grating spectrometer schematic

2.2.2.1 USB4000 spectrometer

The specification of USB4000 spectrometer [16] is listed in table 2.1.

Table2.1: specification of USB4000 spectrometer

Detector	
Detector:	Toshiba TCD1304AP Linear CCD array
Detector range:	200-1100 nm
Pixels:	3648 pixels
Pixel size:	8 μm x 200 μm
Pixel well depth:	100,000 electrons
Signal-to-noise ratio:	300:1 (at full signal)
A/D resolution:	16 bit
Dark noise:	50 RMS counts
Corrected linearity:	>99.8%
Sensitivity:	130 photons/count at 400 nm; 60 photons/count at 600 nm
Spectroscopic	
Wavelength range:	200-850 nm
Optical resolution:	~1.5 nm FWHM
Signal-to-noise ratio:	300:1 (at full signal)
A/D resolution:	16 bit
Dark noise:	50 RMS counts
Integration time:	3.8 ms to 10 seconds
Stray light:	<0.05% at 600 nm; 0.10% at 435 nm
Optical bench	
Focal length:	42 mm input; 68 mm output
Grating:	600 lines (blazed at 300 nm)
Fiber optic connector:	SMA 905 to 0.22 numerical aperture single-strand optical fiber

2.2.2.2 HR4000 spectrometer

The specification of HR4000 spectrometer [17] is listed in table 2.2.

Table2.2: specification of HR4000 spectrometer

Detector	
Detector:	Toshiba TCD1304AP linear CCD array
Detector range:	200-1100 nm
Pixels:	3648 pixels
Pixel size:	8 μm x 200 μm
Pixel well depth:	~100,000 electrons
Sensitivity:	130 photons/count at 400 nm; 60 photons/count at 600 nm
Spectroscopic	
Wavelength range:	200- 400 nm
Optical resolution:	~0.02-8.4 nm FWHM
Signal-to-noise ratio:	300:1 (at full signal)
A/D resolution:	14 bit
Dark noise:	12 RMS counts
Integration time:	3.8 ms to 10 seconds
Stray light:	<0.05% at 600 nm; <0.10% at 435 nm
Corrected linearity:	>99.8%
Optical bench	
Focal length:	101.6 mm input and output
Grating:	1200 Lines Holographic UV
Fiber optic connector:	SMA 905 to 0.22 numerical aperture single-strand optical fiber

2.2.3 Discharge tube

Quartz tube with 15 mm outer diameter, 13 cm inner diameter and 500 mm length was used in the experiment as the discharge tube. One end open and one end closed tube as shown in figure 2.5 was used as discharge tube to study the effect of gas composition, total pressure and rare gases on the emission intensity of UV light.

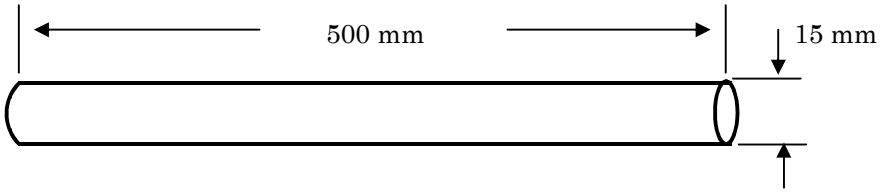

Fig. 2.5: Schematic view of quartz tube

2.3 Experimental procedure

The schematic diagram of the experimental setup for N_2 / O_2 gas discharge is shown in figure 2.6. A quartz tube with 15 mm outer diameter and 500 mm length was used in the

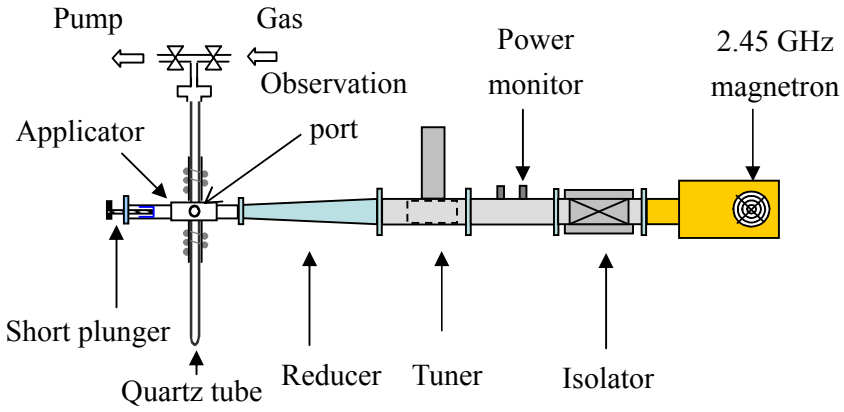

Fig.2.6: Schematic diagram of the experimental set-up

the experiment as the discharge tube. One side of the tube was closed and the other side

was connected to a vacuum system. Rotary pump was used to evacuate the system. The quartz tube was filled with different concentration of N_2 and O_2 gas (both N_2 and O_2 were 99.99995% pure) at various pressure. After filling the tube with gases, microwave power of 100 W was supplied to the applicator. Tesla coil was used for ignition.

Optical emission spectroscopy was carried out using 2 sets of fiber coupled spectrometer, for UV (HR- 4000) and for visible light (USB- 4000) through an observation port consisting of a metal tube with 10 mm inner diameter and 40 mm length on the side wall of the microwave applicator. The optical fiber was set at the end of the port which was 10 cm away from the center of the discharge tube.

2.4 Results and discussion

Figures 2.7(a) and (b) show the emission spectra from pure N_2 microwave plasma in the UV and visible range, respectively. Second positive system existing from 300 to 400 nm is dominant in the UV regions. Peaks in the 2nd positive systems are

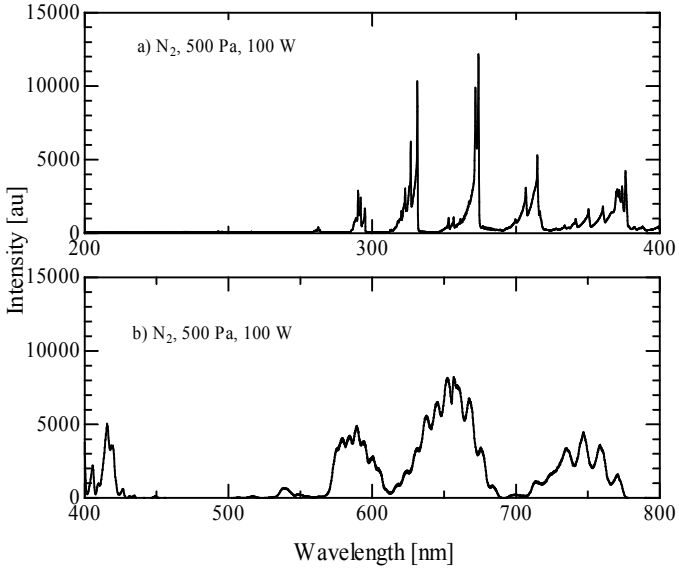

Fig. 2.7: Emission spectra from N_2 (a) in the UV range and (b) in the visible range

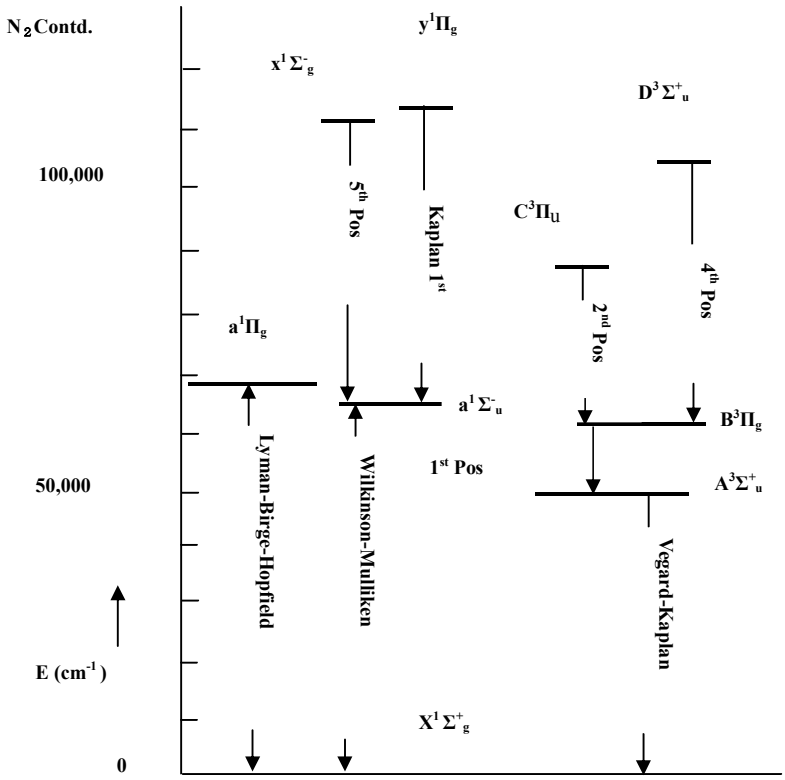

Fig. 2.8: Energy level diagram of N_2 molecule

attributed to the $C^3\Pi_u - B^3\Pi_g$ transition as shown in figure 2.8. The pure N_2 plasma looked bright due to intensive emission in the visible range. These bands are attributed to the 1st positive system through $B^3\Pi_g - A^3\Sigma^+_u$ transition which is also shown in figure 2.8.

Figures 2.9(a) and (b) shows the emission spectra from from N_2/O_2 in the UV range and in the visible range. From figures 2.7(a) and 2.9(a), it is observed that by the addition of O_2, 2nd positive band system decreased whereas some intensive peaks

appeared at 215, 226, 237 and 247 nm. These intensively appeared peaks are from NO

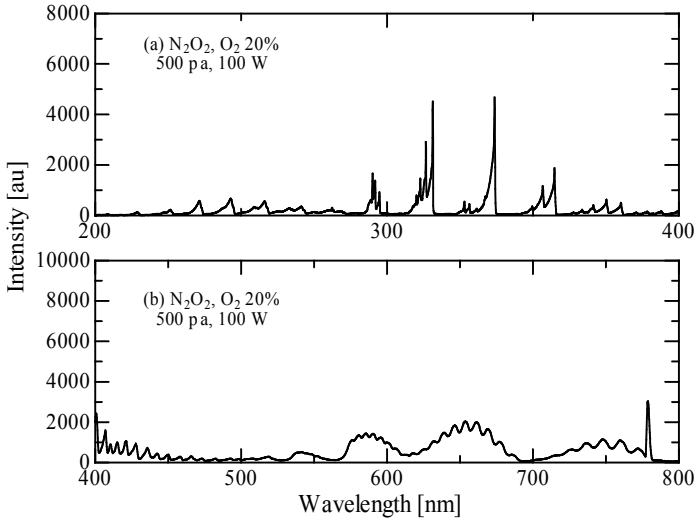

Fig. 2.9: Emission spectra from N_2 /O_2 (a) in the UV range and (b) in the visible range

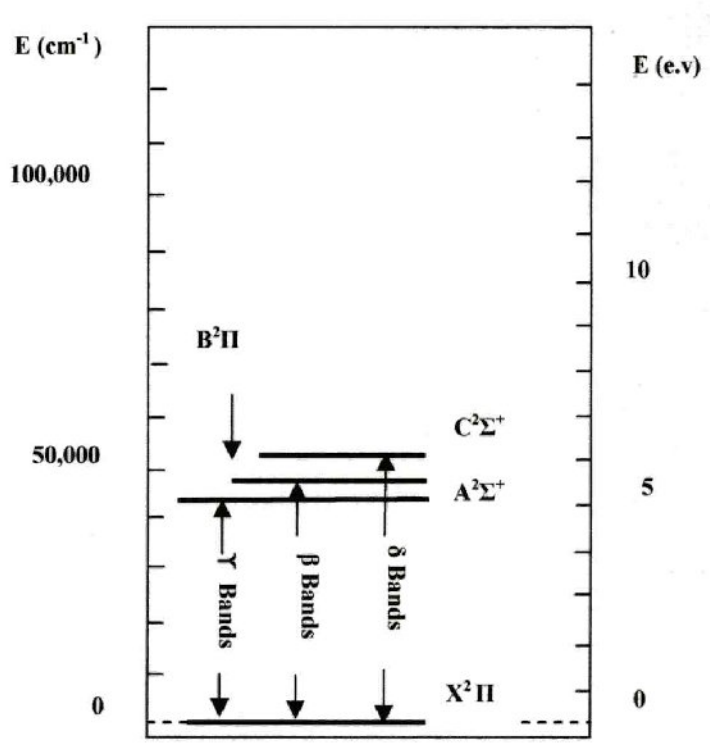

Fig. 2.10: Energy level diagram of NO molecule

γ ($A^2\Sigma^+ - X^2\ \Pi$) system (shown in figure 2.10), which is degraded to the shorter wavelength [18]. As seen from figures 2.7(b) and 2.9(b), the visible emission by 1st positive system dramatically decreased and atomic oxygen peak (777 nm) appeared by O_2 addition.

In N_2/O_2 discharge the dissociation mechanism of nitrogen and oxygen molecules is dominated by electron impact reactions. When nitrogen is mixed with oxygen, dissociation reactions between the ground state oxygen molecules $O_2(X^3\Sigma_g)$ and the excited nitrogen molecules, particularly, $N_2(A^3\Sigma_u)$ state, increases the dissociation of oxygen through the following reaction [19];

$$O_2(X) + N_2(A, B, C, a`) \rightarrow 2O_2(^3P) + N_2(X) \quad \ldots\ldots\ldots\ldots\ldots\ldots\ldots\ldots (1)$$

The oxygen molecules dissociate due to collision with nitrogen molecules.

Concerning nitrogen dissociation, the loss of atomic nitrogen due to collision with oxygen molecules becomes the dominant process for the kinetics of atomic nitrogen. The following reaction is predominant process for the loss of nitrogen atoms and formation of NO molecules [19];

$$N(^4S) + O_2(X) \rightarrow NO + O(^3P) \quad \ldots\ldots\ldots\ldots\ldots\ldots\ldots\ldots\ldots\ldots\ldots\ldots (2)$$

The admixture of oxygen molecules into nitrogen discharge makes the quenching of nitrogen atoms by reaction (2). The dissociation degree of nitrogen becomes small with the increase of oxygen concentration in the discharge. The dissociation degree of both nitrogen and oxygen increases with nitrogen concentration. The dissociation of oxygen is enhanced by nitrogen admixture due to collisions with the excited nitrogen molecules, particularly with $N_2(A^3\Sigma_u)$ state. In case of nitrogen dissociation, the dissociated

nitrogen atoms are frequently lost by collisions with oxygen molecules and form NO molecules.

2.4.1 Optimization of pressure and gas composition

Discharge was produced at different concentration of O_2 and N_2 gas and at different total pressure. Figure 2.11 shows the variation of intensity of 247 nm peak with total pressure and gas composition. From the figure, it can be seen that, at 100 Pa pressure the intensities of 247 nm peak was lowest for all different gas composition except 50% O_2 and 50% N_2. On the other hand, at 500 Pa pressure, the intensities were highest for all the gas composition. The intensities at 1 kPa and 2 kPa and at different gas composition were in between intensities produced at 100 Pa and 500Pa.

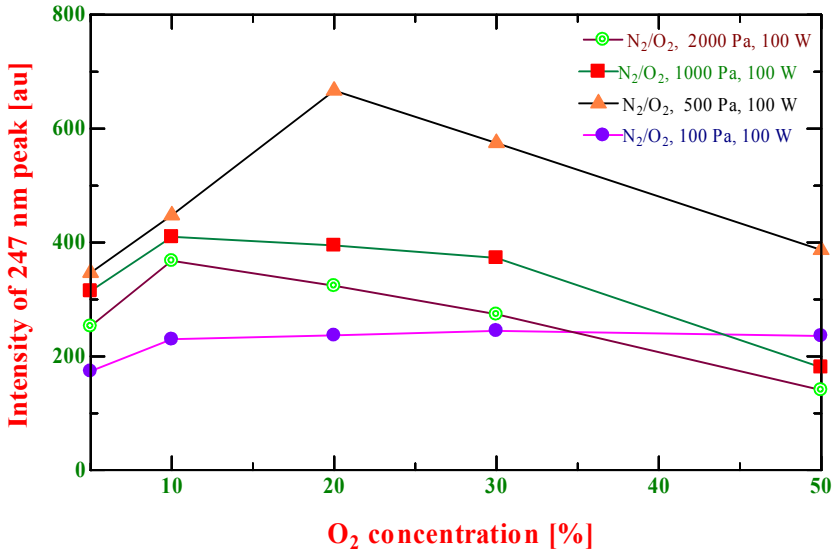

Fig. 2.11: Variation of Emission intensity with total pressure and gas composition.

It is clear from the figure that the intensity is highest at 500 Pa and 20% O_2.

The reason for the enhancement at this composition and pressure is that the dissociation degree of nitrogen is maximum at this composition and pressure [19]. This dissociated nitrogen atoms form NO molecules by collision with oxygen through the following reaction

$$N(^4S) + O_2(X) \rightarrow NO + O(^3P) \quad \ldots\ldots\ldots\ldots\ldots (3)$$

2.4.2 Optimization of power

The variation of intensity of 247 nm peak with applied power is shown in figure 2.12. From the figure it is clear that the intensity increased sharply when applied

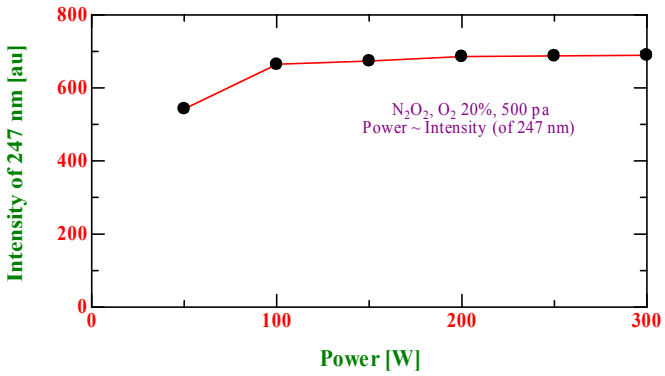

Fig. 2.12: Dependence of emission intensity on applied power.

power is increased from 50 W to 100 W. When the power is increased further up to 300W, the intensity is slightly increased. At 50 W applied power, it was difficult to start the discharge. On the other hand, when the applied power was 150 W and above that, the MW applicator became very hot within short time after the starting of discharge. So applied power of 100 W was used as the optimized power in the experiment to avoid heating problem and to start the discharge easily.

2.5 Emission spectra from NO discharge

Emission spectra from NO discharge in the UV range at different pressure is presented in figure 2.13. Many high intensity emission lines in the 200 to 300 nm region of the plasma originated from nitrogen monoxide (NO). The emission system was identified as the γ band ($A^2\Sigma^+ - X^2\Pi$) of NO. Some other high intensity emission lines appeared at 295, 316, 337 and 357 nm. These peaks are from 2nd positive band ($C^3\Pi_u - B^3\Pi_g$) system of N_2.

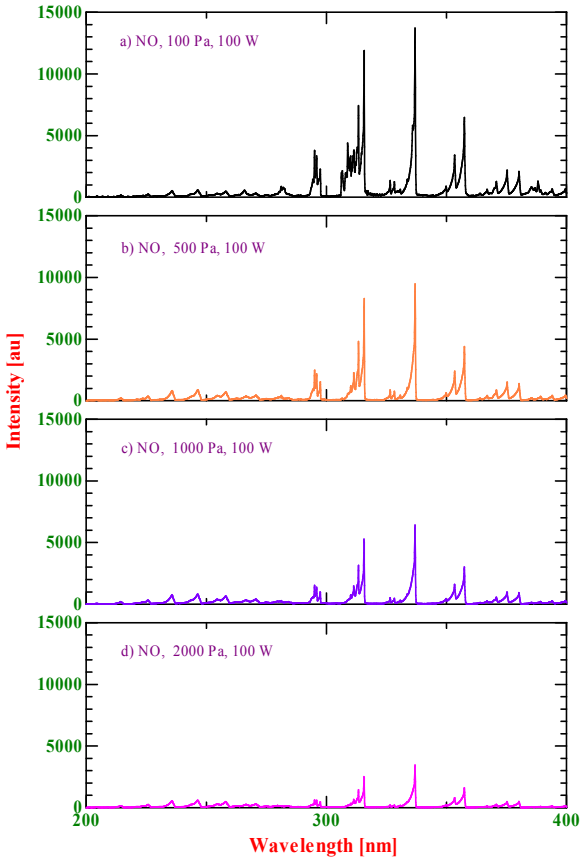

Fig. 2.13: Emission spectra in the UV range from NO discharge at different pressure.

Figure 2.14 shows the emission spectra fro NO discharge in the visible region.

The emission spectra in the visible region was identified as 1st positive band ($B^3\Pi_g - A^3\Sigma^+_u$) of N_2. A high intensity emission line from atomic oxygen was also observed at 777 nm. During NO discharge, NO decomposes into N_2 and O_2 as follows

$$NO \rightarrow N_2 + O_2 \quad \ldots\ldots\ldots\ldots\ldots\ldots \quad (4)$$

The emission lines from 1st and 2nd positive bands of N_2 are due to the decomposed N_2. Similarly the atomic oxygen line is also produced from the decomposed O_2.

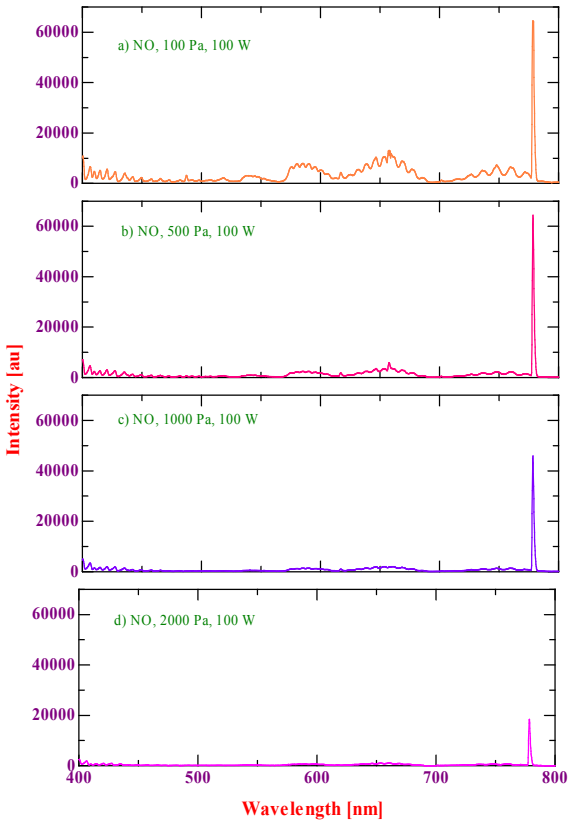

Fig. 2.14: Emission spectra in the visible range from NO discharge at different pressure.

2.6 Summary

N_2/O_2 mixture microwave discharge emits intensive UV light in the 200 to 280

nm region through NO $\gamma(A^2\Sigma^+ - X^2\Pi)$ system.

Emission intensity in the UV region varies with gas composition. The highest intensity was obtained at 80% N_2 and 20% O_2 concentration.

UV emission intensity also changes with total pressure. The intensity was highest at 500 Pa total pressure.

References

[1] Yu. A. Lebedev, High Temperature, **45,** 134–136 (2007).

[2] A. Didenko, B.Zverev, A.Koljaskin, A. Ponomarenko and A. Prokopenko, Proc. IV Int. work, Microwave discharges: Fundamentals and applications, 22 (2000).

[3] A. Kozlov, V. Perevodchikov, R. Umarhodzaev and E. Shlifer, Proc. IV Int. work, Microwave discharges: Fundamentals and applications, 27 (2000).

[4] K.F. Sergeichev, I.A. Sychov and D.V. Vlasov, Proc. IV Int. work, Microwave discharges: Fundamentals and applications, 25 (2000).

[5] O. Matsumoto, K.Itoh and Y. Takhasi, Proc. IV Int. work, Microwave discharges: Fundamentals and applications, 23 (2000).

[6] A.L. Vikharev: Proc. IV Int. work, Microwave discharges: Fundamentals and applications, 26 (2000).

[7] M. Moisan and Z. Zakrzewski, Plasma Sources Sci. Technol., **4**, 379–97 **(**1995).

[8] J. P. J.Van Dalen, P. A. De Lezenne Coulander and L. De Galan, Spectrochemica Acta, **33a,** 545–549 (1977).

[9] V. Ibberson, Microwave plasma techniques, New Scientist, **103**, 1414-1426 (1984).

[10] D. Kalluri and R. Prasad, Plasma Sci., **6,** 568–73 (1978).

[11] A. Kraszewski, Microwave Gas Discharge Devices, Iliffe, 2nd edition (1967).

[12] J. D. Ametepe, J. Diggs, D.M. Manos and M. J. Kelley, J. Appl. Phys., **85,** 7505–7510 **(**1999).

[13] A. I. Al-Shamma, I. Pandidas and J. Lucas, J. Phys. D: Appl. Phys., **34,** 2775 (2001).

[14] A. Kono, J. Wang and M. Aramaki, Thin Solid Films, 506-507 (2006).

[15] A. C. Fozza, A. Kruse, A. Hollдnder, A. Ricard and M. R. Wertheimer, J. Vac. Sci. & Technol., **16**, 72 (1988).

[16] Installation and Operation Manual: USB4000 Fiber Optic Spectrometer.

[17] Installation and Operation Manual: HR4000 and HR4000CG-UV-NIR Series High-Resolution Fiber Optic Spectrometers.

[18] R. W. B. Pears and A. G. Gaydon, Identification of Molecular Spectra, Chapman and Hall Ltd., London (1984).

[19] Y. Ichikawa, T. Sakamoto, H. Matsuura and H. Akatsuka, Proc., 5th Asia Pacific Int. Sym. On basics and application of plasma technol., 74-77 (2007).

Chapter 3

Effect of rare gas admixture and pulse operation on N_2/O_2 gas mixture discharge

Introduction

In gas discharge, admixture of rare gases with other gases is a common technique for realizing the desired condition for application. Sakamoto et al. examined the effect of rare gas admixture with oxygen discharge on the vibrational and rotational temperatures of the OH radical by optical emission spectroscopy (OES). They used helium, neon, argon, krypton and xenon as admixture components with oxygen [1]. S. Gortchakov and D. Uhrlandt studied glow discharges in mixtures of xenon with other rare gases aiming to use it for mercury free UV light source to replace the mercury UV lamp [2]. N. D. Smith measured the intensity distribution of continuous spectrum of hydrogen by admixture of rare gases (He and Ne). The effect of these gases was to shift the maximum of intensity to longer wavelength [3]. Fozza et al. investigated the VUV to near infrared emissions from molecular gas–noble gas mixtures (H_2–Ar and O_2–Ar) to obtain very intense VUV emissions to apply it for the photochemical treatment of polymer surface [4]. The effect of gas composition on spore mortality has been investigated by Lerouge et al. using gases such as pure O_2, O_2/CF_4 and O_2/Ar [5]. S Kitsinelis et al. studied of spectral output with a range of different buffer gases (neon, argon, krypton and mixtures of these gases) [6]. It was observed that near-UV output is maximized when argon is used.

In this chapter, the effect of rare gas admixture with N_2/O_2 gas has been discussed. Experiment to study the effect of inert gases on the intensity of the emission was carried out. He, Ne, Ar, Kr and Xe gases were used at different percentages of concentration. It was observed that at low concentration below 5%, these gases have no effect on the emission intensity whereas the emission intensity in both the UV and visible ranges decreased as the rare gas concentration was increased. The gases behave as buffer gases. Buffer gases caused collisions with the other co-existing molecules and decreases the emission intensity.

The effect of pulse operation on N_2 /O_2 discharge has also been discussed in this chapter.

3.1 Experimental method

The schematic diagram for the experiment is shown in figure 3.1. A quartz tube with 13 mm inner diameter and 500 mm length was used in the experiment as the

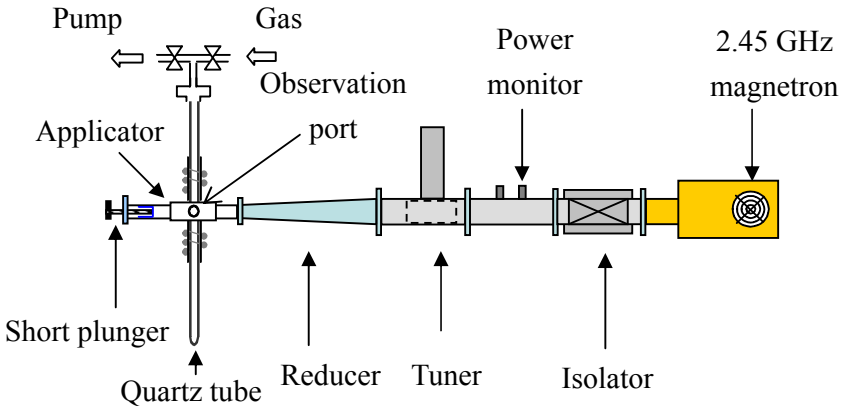

Fig. 3.1: Schematic diagram of the experiment

discharge tube. The discharge tube was inserted into the MW applicator. One side of the

tube was closed and the other side was connected to a vacuum system. Rotary pump was used to evacuate the system. The total pressure in the tube was measured by Baratron pressure gauge (Type 626).

The quartz tube was filled with different concentration of N_2, O_2 and rare gases (He, Ne, Ar, Kr and Xe) at various pressure. After filling the tube with gases MW power of 100 W was applied to produce discharge. Tesla coil was used for ignition. Reflected power was adjusted to 0 W by means of tuner. Emission spectroscopy was carried out using 2 sets of fiber coupled spectrometer, through an observation port on the side wall of the microwave applicator. The optical fiber was set at the end of the port which was 10 cm away from the center of the discharge tube.

During the pulse operation the interval and width of the pulse were varied. Emission spectroscopy was carried out as the same way discussed above.

3.2 Effect of Ar admixture

N_2/O_2/Ar discharge was produced at different concentration of O_2, N_2 and Ar gas to investigate the effect of Ar admixture on the UV intensity emitted from N_2/O_2 discharge. Figure 3.2 and 3.3 show the emission intensity at different gas composition in the UV and visible range respectively. It can be seen from figure 3.2 that UV emission intensity changes with Ar concentration. However the shape and peak position remain same in the UV region up to 50% of Ar concentration. At 2% O_2, and 90% Ar, no emission was observed in the UV region. From figure 3.3, it is seen that emission intensity in the visible range also changes with Ar concentration. In the visible region, some additional peaks (at 698, 708, 739, 752 and 764 nm) from Ar were observed at

high concentration of Ar. As the concentration of Ar increased the peaks also increased.

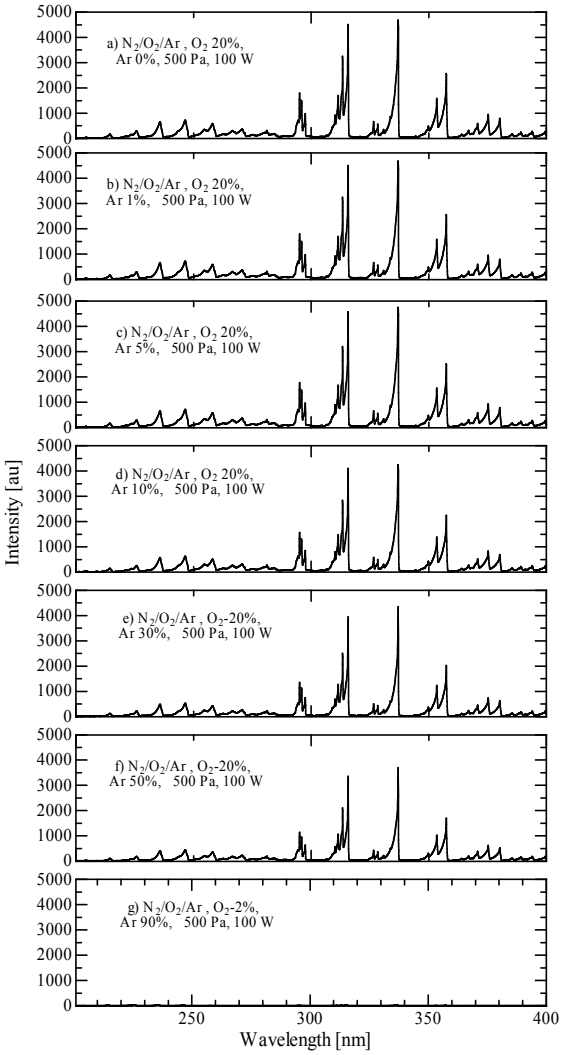

Fig. 3.2: Emission spectra from N_2/O_2 /Ar microwave discharge at various Ar concentration

It was observed from both figure 3.2 and figure 3.3 that at low concentration below 5%, Ar gas has no effect on the emission intensity. However the emission intensity in both the UV and visible ranges decreased as Ar gas concentration was

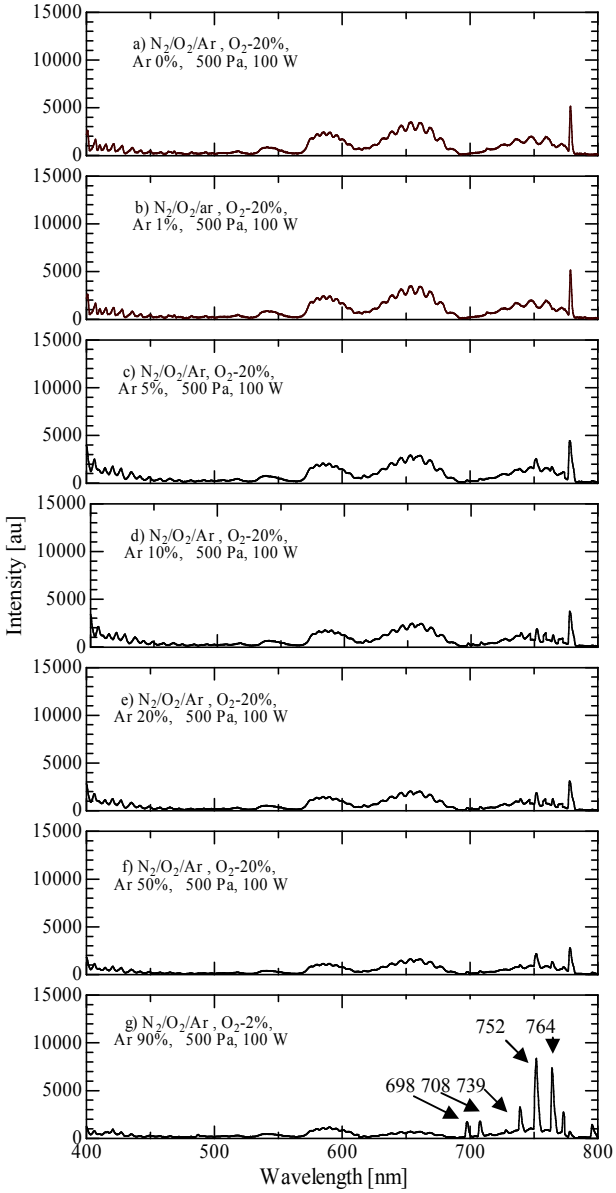

Fig. 3.3: Emission spectra from N_2/O_2 /Ar microwave discharge in the visible range at various concentration of Ar

increased above 5%. The reasons for the decrease of intensity can be explained as

following. As mentiond in chapter 2, the UV intensity emitted from NO molecule is maximum at 80% N_2 and 20% O_2 [7]. Below this concentration of N_2, the intensity decreased. When we increased Ar concentration, N_2 concentration decreased in the gas mixture and so the emission intensity also decreased with increasing Ar concentration. Emission in the 300- 400 nm range is from 2^{nd} positive system of N_2. In previous chapter (chapter 2) it was also observed that the intensity in this range decreased with decreased concentration of N_2. In case of N_2 /O_2 /Ar discharge, as the concentration of N_2 decreased with the increase of Ar concentration, the emission intensity within this region also decreased. The emission intensity in the visible region which is from 1^{st} positive system of N_2 also decreased when N_2 concentration is decreased. So in N_2 /O_2 /Ar discharge the intensity of emission also decreased for the same reason as mentioned earlier. The other reason for the decrease of intensity in both UV and visible range is that Ar gas behaves as buffer gas in the mixture. Buffer gases caused collisions with the other co-existing molecules and decreases the emission intensity.

3.3 Effect of Kr admixture

Figure 3.4 and 3.5 show the emission intensity from N_2/O_2/Kr discharge at different gas composition in the UV and visible range respectively. From figure 3.4 it was observed that the shape and peak position remained same in the UV region although emission intensity in this range changed with Kr concentration. In the visible region (as shown in figure 3.5), emission intensity also changed with Kr concentration and some additional peaks from Kr appeared at high concentration of Kr.

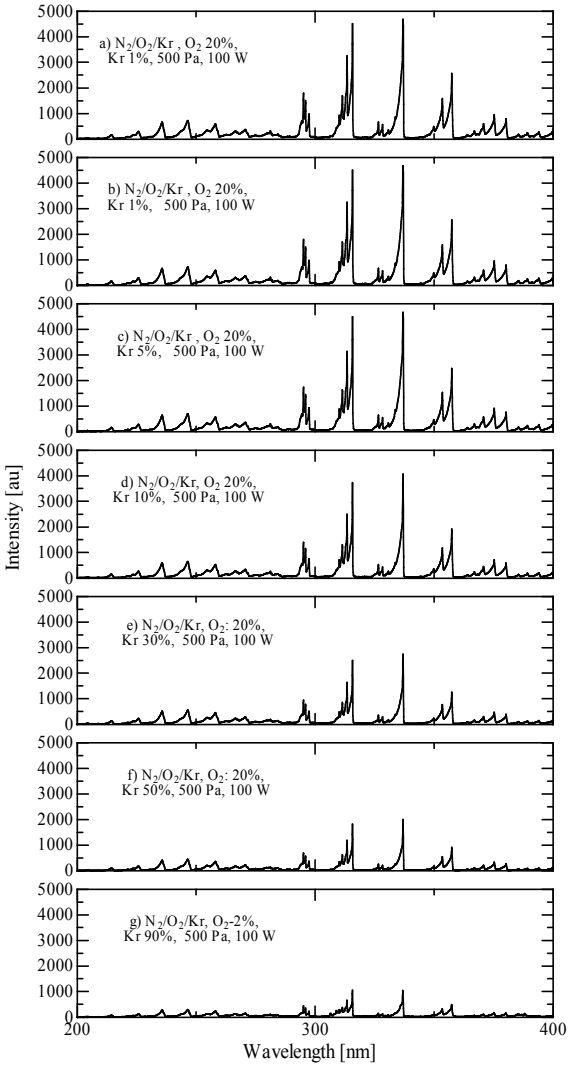

Fig. 3.4: Emission spectra from N_2/O_2 /Kr microwave discharge at various Kr concentration

The admixture of Kr showed almost the same effect as of Ar. Below 5% concentration, Kr has also no effect on the emission intensity. However above 5% of concentration, the emission intensity in both the UV and visible ranges decreased. The reasons for the

decrease of intensity are same as mentioned in case of Ar admixture.

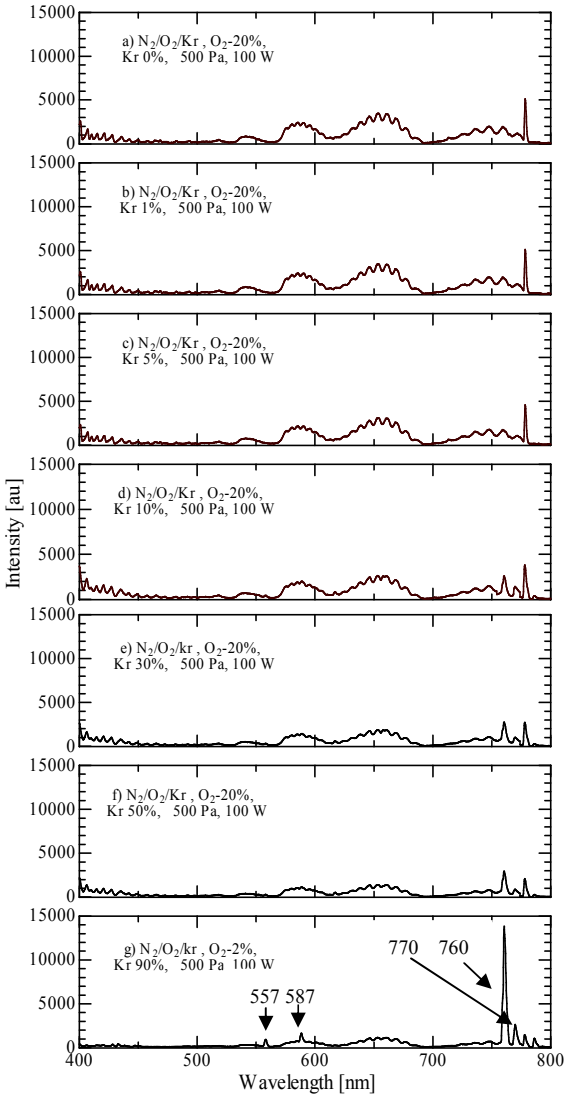

Fig. 3.5: Emission spectra from N_2/O_2 /Kr microwave discharge in the visible range at different concentration of Kr

3.4 Effect of Xe admixture

The effect of Xe admixture on the emission intensity emitted from N_2/O_2

discharge in the UV and visible range is shown in figure 3.6 and 3.7 respectively. From figures 3.6 and 3.7, it has been observed that admixture of 1% xe has no effect on the

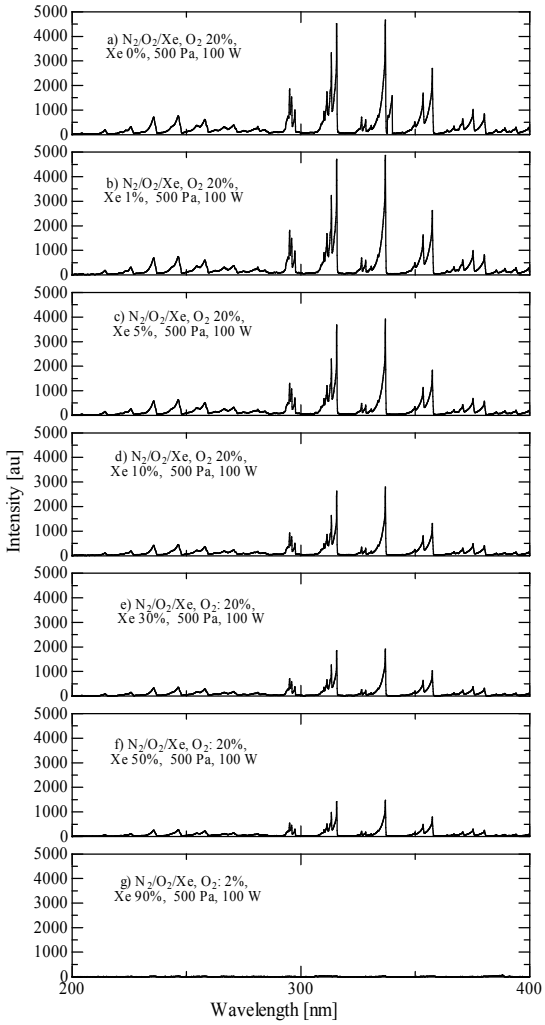

Fig. 3.6: Emission spectra from N_2/O_2 /Xe microwave discharge at various Xe concentration

emission intensity in both UV and visible region. However at 5% and above this concentration the intensity gradually decreased. It is also observed that (from figure

3.7) at higher concentration of Xe some additional peaks from Xe at 467, 492 and 713 nm appeared in the spectrum.

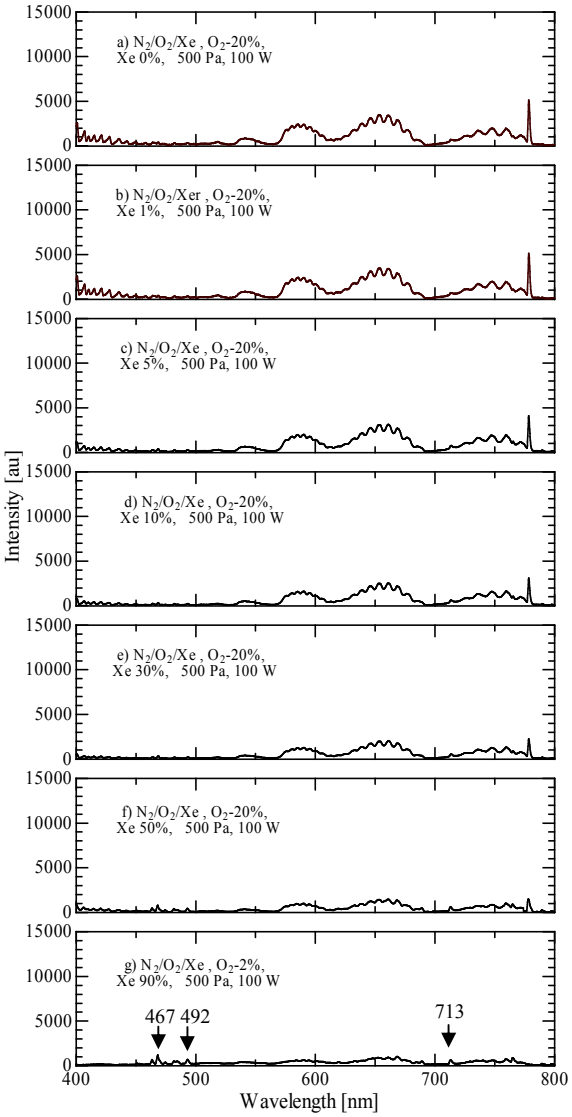

Fig. 3.7: Emission spectra from N_2/O_2 /Xe microwave discharge in the visible range at different Xe concentration

3.5 Effect of He admixture

Figures 3.8 and 3.9 show the effect of He admixture on the emission intensity emitted from N_2/O_2 discharge in the UV and visible range respectively. Figure 3.8 shows that the emission intensity changed with He concentration but the peaks position remained same in the UV range. In the visible region, the intensity gradually decreased with increased He concentration an at 90% He and 2% O_2 concentration, He peaks at 487 and 747 nm were observed.

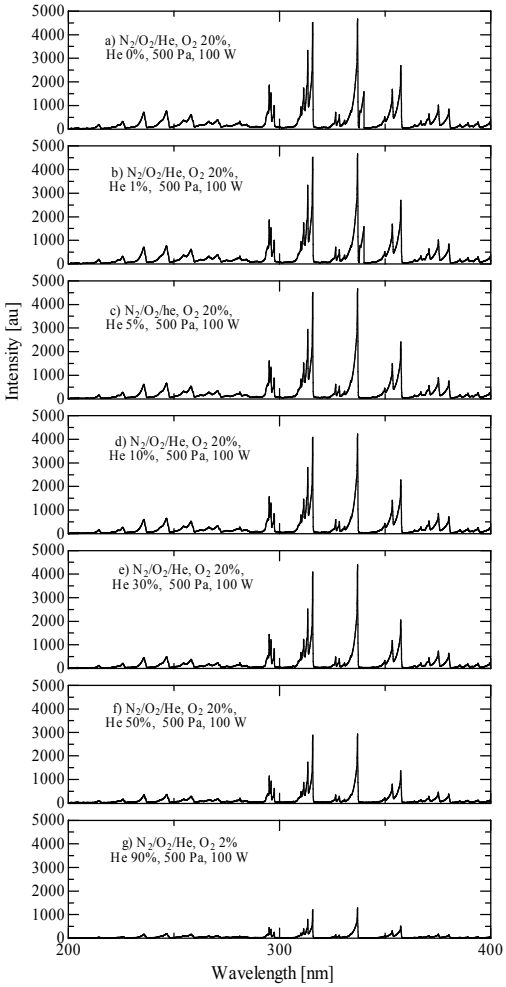

Fig. 3.8: Emission spectra from N_2/O_2 /He microwave discharge at various concentration of He

The one reason for the decrease of intensity is the decrease of N_2 concentration with the increase of rare gas concentration in the mixture and the other reason is the behavior of He gas in the mixture as buffer gas. Buffer gases caused collisions with the other co-existing molecules and decreases the emission intensity.

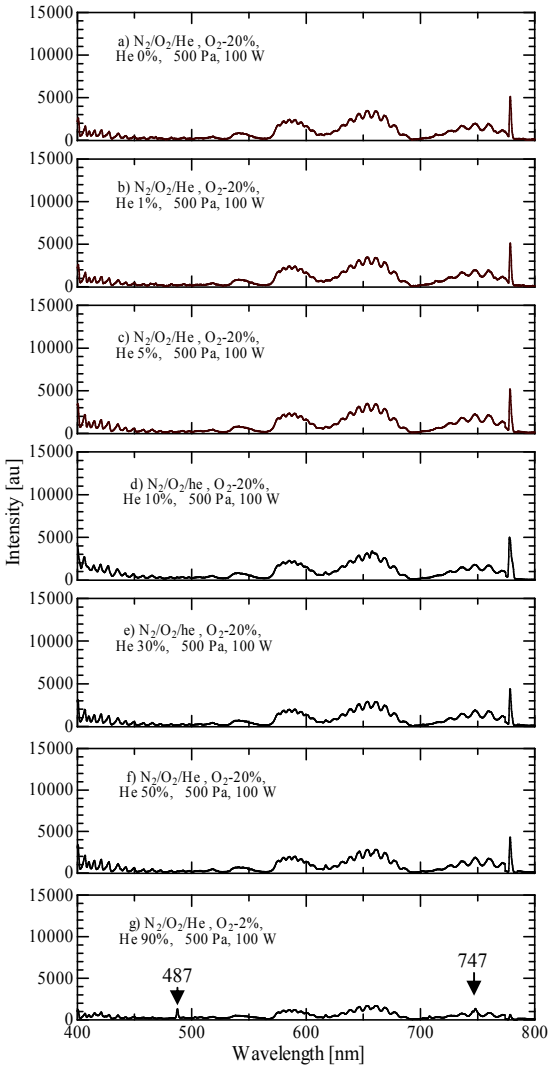

Fig. 3.9: Emission spectra from N_2/O_2 /He microwave discharge in the visible range at different He concentration

3.6 Effect of Ne admixture

Figure 3.10 shows the effect of Ne admixture on the emission intensity in the UV region and figure 3.11 shows the effect of Ne admixture on the emission intensity in the UV region emitted from N_2/O_2 discharge.

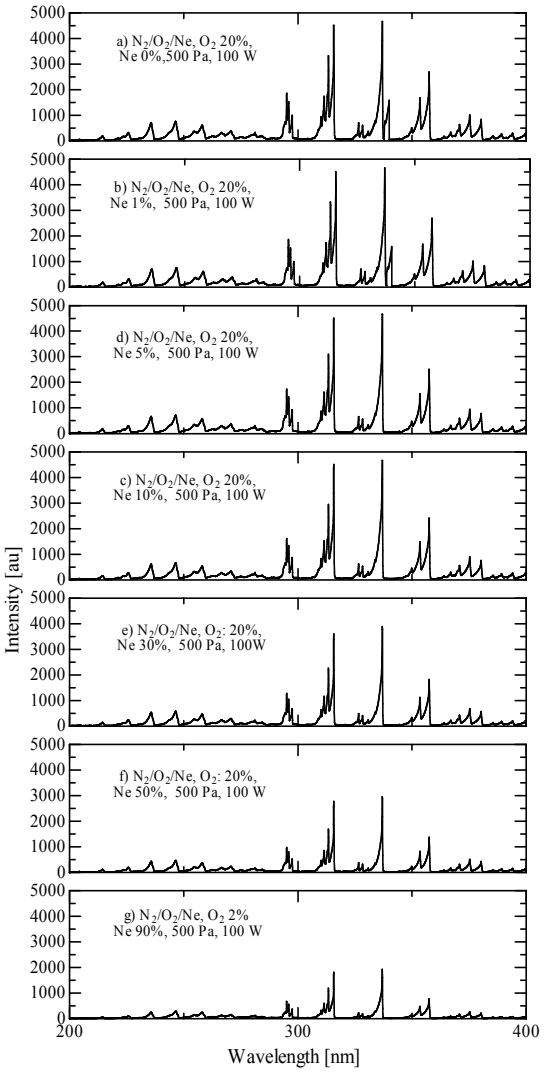

Fig. 3.10: Emission spectra from N_2/O_2 /Ne microwave discharge at various concentration of Ne

It is seen from figures 3.10 and 3.11 that admixture of 1% Ne has no effect on the emission intensity in both UV and visible region. However at 5% and above this concentration the intensity gradually decreased. From figure 3.11, it is also observed that at 90% Ne and 2% O_2 concentration, Ne peaks appeared at 488, 585 and 659 nm.

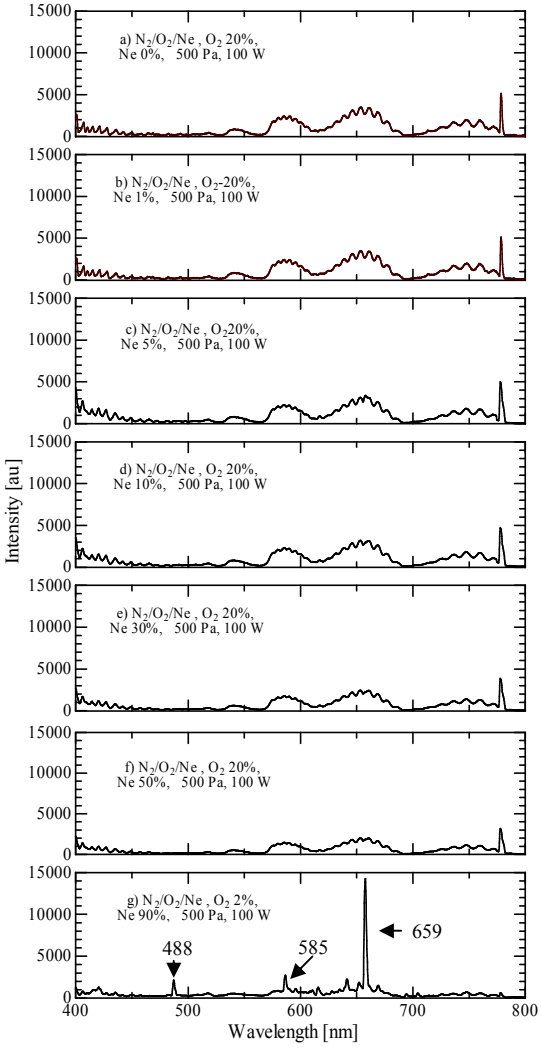

Fig. 3.11: Emission spectra from N_2/O_2 /Ne microwave discharge in the visible range at different Ne concentration

3.7 Effect of pulse operation

The dependence of pulse width and pulse interval on the intensity of the UV emission emitted from N_2/O_2 discharge was studied.

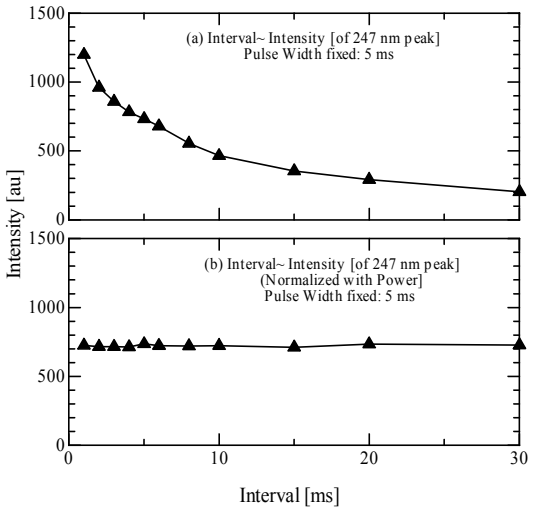

Fig.3.12: Dependence of pulse interval on emission intensity of N_2/O_2 discharge (a) interval ~ intensity and (b) interval ~intensity [normalized with power]

The dependence of pulse interval on emission intensity is shown in Fig. 3.12. From Fig. 3.12(a), it can be seen that intensity decreases with the increase of interval. This happens because with the increase of pulse interval, the duty decreases and hence the applied power. From Fig. 3.12(b) it is clear that emission intensity does not depend on pulse interval but depends on power.

Figure 3.13 shows the effect of pulse width on emission intensity. It is observed from Fig. 3.13(a) that intensity increases when pulse width is increased. This happens because duty increases with the increase of pulse width and so the power. It can be seen

from Fig. 3.13(b) that the emission intensity completely depends on average applied power but not on pulse width.

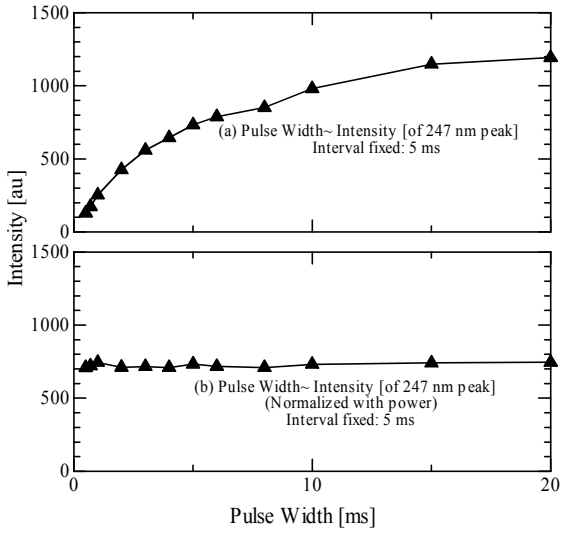

Fig.3.13: Dependence of pulse width on emission intensity of N_2 /O_2 discharge (a) pulse width ~ intensity and (b) pulse width ~intensity [normalized with power]

Pulse interval from 30 ms to 1 ms was used in the experiment. Figure 3.12(b) shows that there is no variation of intensity due to the variation of pulse interval. This indicates that there is no accumulation of NO molecules from the duration of one pulse interval to the next pulse interval. Therefore, it can be concluded that the life time of NO molecule is shorter than 1 ms.

3.8 Summary

He, Ne, Ar, Kr and Xe gases at different percentages of concentration was used in the experiment to examine the effect of theses gases on the emission intensity emitted from N_2 /O_2 discharge. It was observed that at low concentration below 5%, these gases

have no effect on the emission intensity whereas the emission intensity in both the UV and visible ranges decreased as the rare gas concentration was increased. The gases behave as buffer gases. Buffer gases caused collisions with the other co-existing molecules and decreases the emission intensity. The other reason for the decrease of intensity is the decrease of N_2 concentration with the increase of rare gas concentration in the mixture.

UV intensity in 200- 400 nm region does not vary with pulse width and pulse interval but depends on average power. The life time of NO molecules is shorter than 1 ms.

References

[1] T. Sakamoto, K. Naoi, H. Matsura and H. Akatsuka, Jpn. J. Appl. Phys., **45**, 243–246 (2006).

[2] S. Gortchakov, D. Uhrlandt, XXVI Int. Con. on Phenomena in Ionized Gases, 45 (2003).

[3] N. D. Smith, Physical review, **49**, 345-350 (1936).

[4] A. C. Fozza, A. Kruse, A. Hollдnder, A. Ricard and M. R. Wertheimer, J. Vac. Scie. & Technol., **16**, 72 (1988).

[5] S. Lerouge, M. R. Werttheimer, R. Marchand, M. Tabrizian and L'H. Yahia, J. Biomed. Mater. Res., **51,** 128 (2000).

[6] S Kitsinelis1, R Devonshire1, M Jinno1, K H Loo2, D A Stone2 and R C Tozer, J. Phys. D: Appl. Phys., **37,** 1630–1638 (2004).

[7] Y. Ichikawa, T. Sakamoto, H. Matsuura and H. Akatsuka, Proc., 5th Asia Pacific Int. Sym. On basics and application of plasma technol., 74-77 (2007).

Chapter 4

Long time operation of microwave excited N_2/O_2 gas mixture discharge

Long time operation of microwave excited N_2 /O_2 gas mixture discharge without refreshing the enclosed gas is discussed in this chapter. After a few hours of operation, the spectrum emitted from N_2 /O_2 discharge changed not due to chemical reaction but due to increased pressure through leakage of the system. So separate closed tube was prepared to examine life time. Microwave power was used for excitation of discharge to avoid degradation of molecular gases through chemical reactions with electrodes. The result showed that the concentration of O_2 decreased with time and so the UV intensity from NO also decreased. It was also observed that after several 10 hours of operation, the partial pressure of N_2 decreased and eventually the discharge stopped.

4.1 Experimental method

Two sets of experiment were carried out. One was “closed tube” experiment and the other was “gas controlled tube” experiment. The schematic view of the “closed tube” experiment is presented in figure 4.1. The microwave source used in the experiment was a magnetron power source operating at 2.45 GHz. The power to the applicator was fed through a rectangular waveguide from the microwave source.

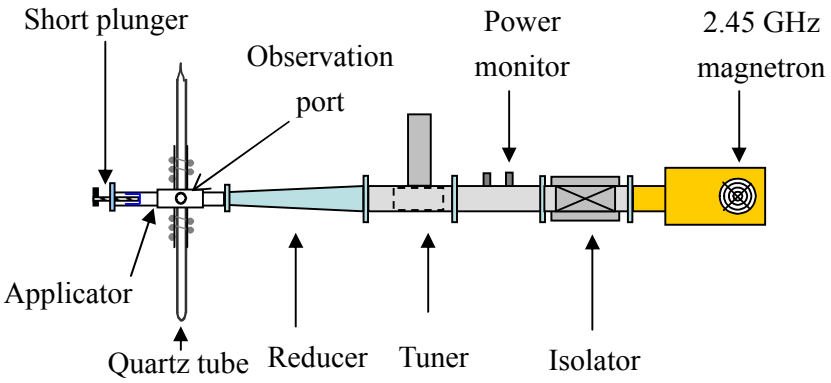

Fig. 4.1: Schematic view of the “closed tube” experiment

A closed quartz tube with 13 mm inner diameter and 500 mm length was used in the experiment. The quartz tube was evacuated in an oven to eliminate out gasing and filled with N_2 and O_2 gas (both N_2 and O_2 were 99.99995% pure). The partial pressure of N_2 was 400 Pa and the partial pressure of O_2 was 100 Pa, resulting in oxygen concentration 20%. After filling the gas, the quartz tube was closed using a burner.

In the "gas controlled tube” experiment (as shown in figure 4.2), a quartz tube with same inner diameter (13 mm) and length (500 mm) as the closed tube was used. One side of the tube was closed and the other side was connected to a vacuum system and gas line. Rotary pump was used to evacuate the system. The quartz tube was filled with different concentration of N_2 and O_2 gas (both N_2 and O_2 were 99.99995% pure) at various pressure. The pressure in the tube was measured by Baratron pressure gauge (Type 626). The same microwave power source was used in both the experiment.

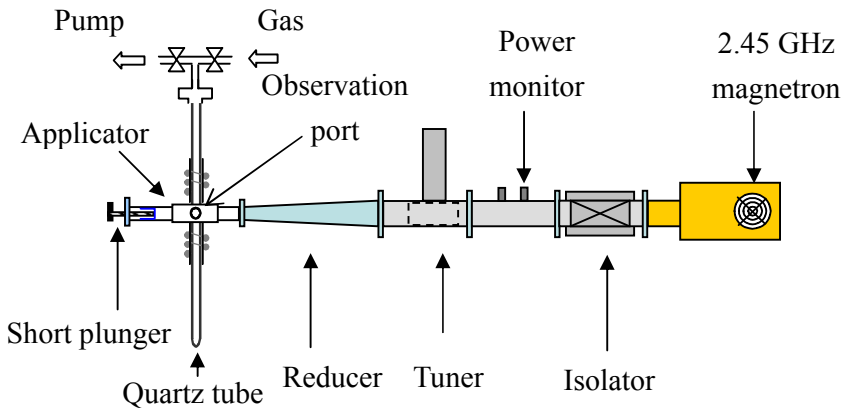

Fig. 4.2: Schematic view of the "gas controlled tube" experiment

Emission spectroscopy was carried out using 2 sets of fiber coupled spectrometer, for UV (HR4000) and for visible light (USB4000) through an observation port on the side wall of the microwave applicator. The optical emission from the central part of the discharge tube was monitored. In closed tube experiment, emission spectroscopy was carried out at every 30 minutes whereas in gas controlled experiment, emission spectroscopy was carried out shortly after the starting of discharge.

4.2 Results and discussion

Figures 4.3(a) and (b) show the emission spectra from N_2/O_2 microwave (100 W) discharge plasma produced in the "closed tube" in UV and visible range, respectively. Emission from 2^{nd} positive system of N_2 is dominant in the 300- 400nm

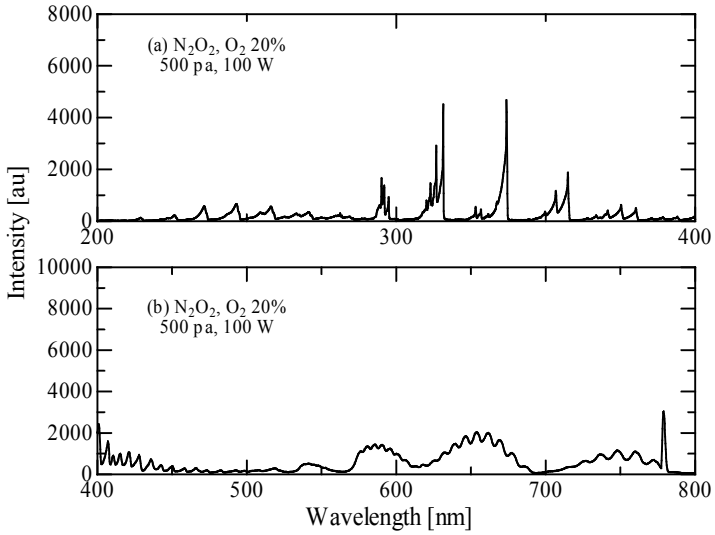

Fig. 4.3: Emission spectra from $N_2 + 20\%$ O_2 (a) in the UV range and (b) in the visible range.

region whereas the emission in the 200- 300 nm range is from NO γ system. Peaks in the 2nd positive systems (of N_2) are attributed to the $C^3\Pi_u - B^3\Pi_g$ transition. In the 200- 300 nm range, intensive peaks appeared at 214, 225, 236 and 247 nm. These intensively appeared peaks are from NO $\gamma(A^2\sum^+ - X^2\Pi)$ system, which is degraded to the shorter wavelength [1]. The emission bands in the visible region are attributed to the 1st positive system of N_2 through $B^3\Pi_g - A^3\sum_u^+$ transition.

Figure 4.4 shows the emission spectra in the visible range emitted from N_2/O_2 gas mixture microwave discharge at different O_2 concentration in the "gas controlled tube" experiment. It is observed from these figures that intensity of O_2 peak increases with the increase of O_2 concentration in the gas mixture.

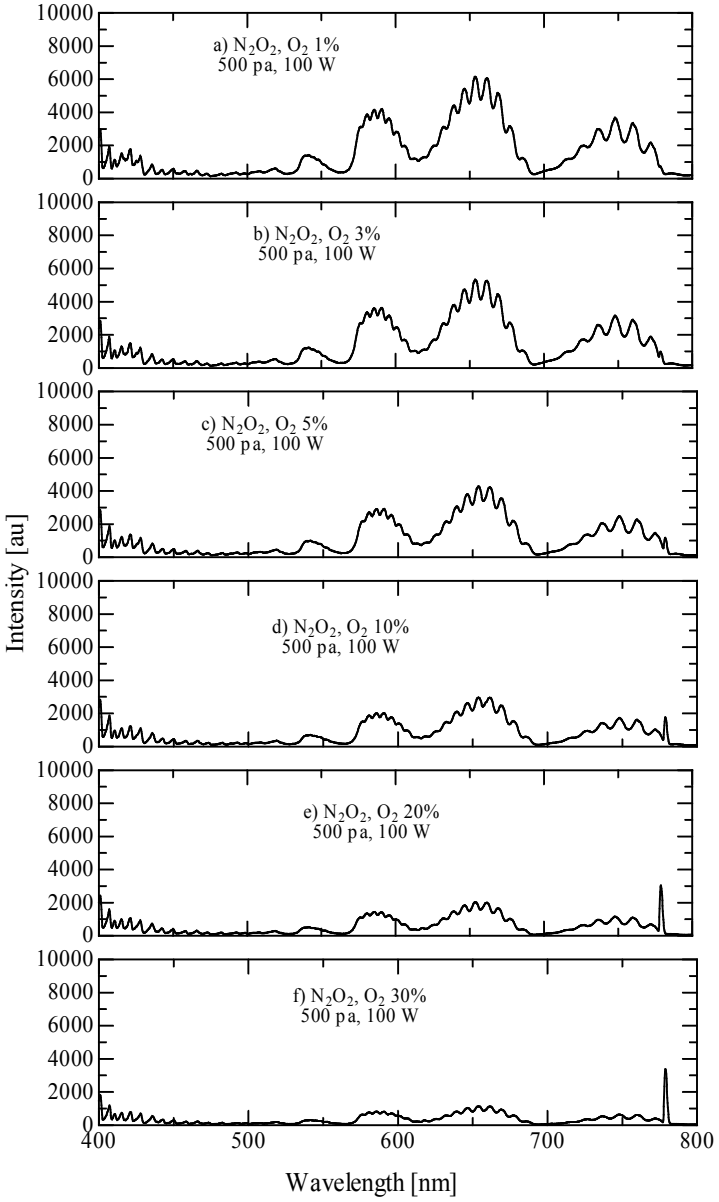

Fig. 4.4: Emission spectra from N_2/O_2 microwave discharge at various O_2 concentration.

The time dependence emission spectrum in the visible range from the "closed tube" experiment is shown in figure 4.5. It can be seen from the figures that, intensity of O_2 peak decreases with operation time indicating that O_2 concentration in the discharge tube decreases with time.

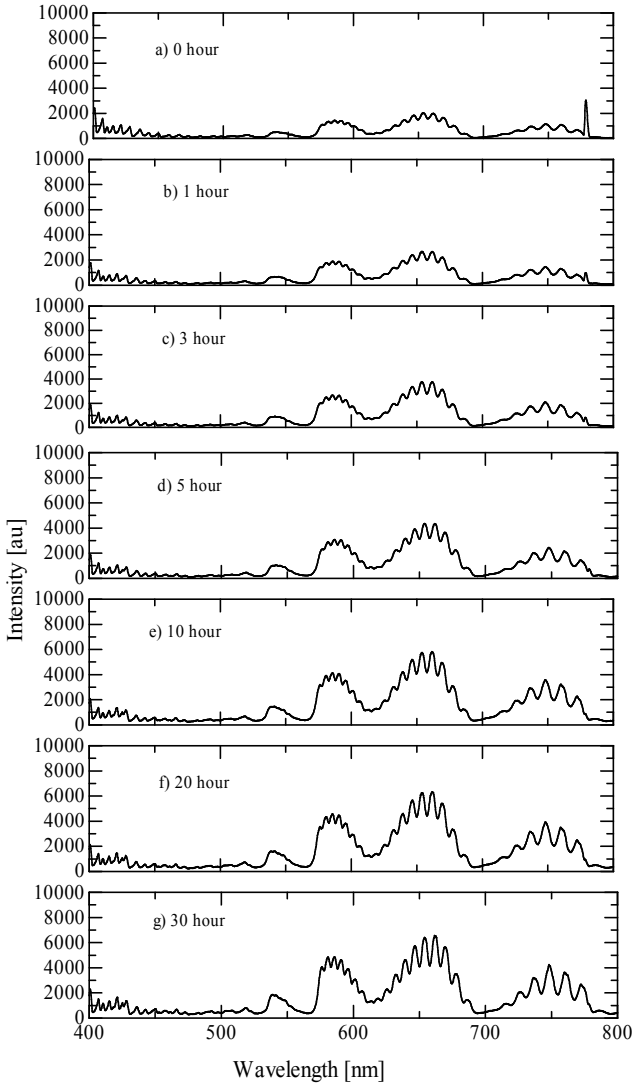

Fig. 4.5: Time dependent emission spectra from N_2/O_2 microwave discharge in "closed tube" experiment.

Figure 4.6(a) shows the emission intensity of oxygen atomic peak (777 nm) from

"gas controlled tube" with variation of O_2 concentration and figure 4.6(b) presents the emission intensity of oxygen atomic peak from "closed tube" with continuous operation. From figure 4.6(a), it can be seen that the intensity of oxygen atomic peak increased with the increase of O_2 concentration. On the other hand, figure 4.6(b) shows that the emission intensity of oxygen atomic peak rapidly decreased for first 1

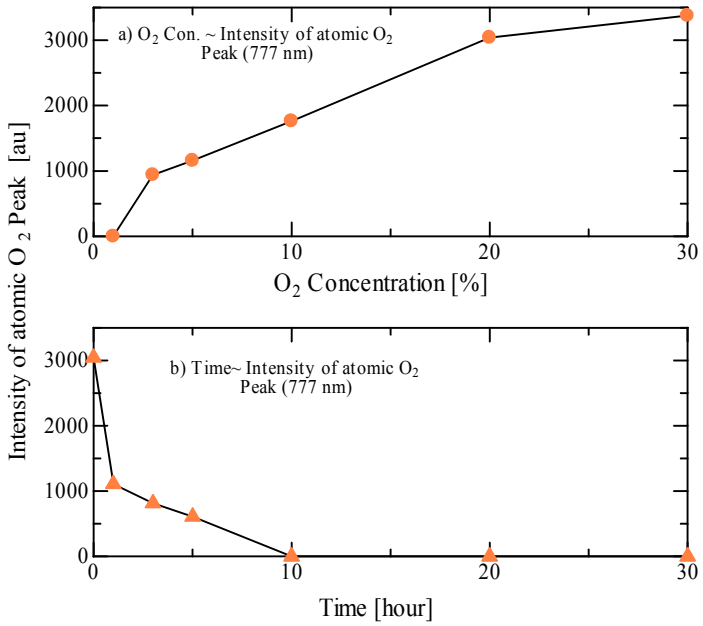

Fig. 4.6: Variation of intensity of atomic O_2 peak (777 nm) with (a) O_2 concentration (pressure 500 Pa) and (b) Time. Microwave power was 100 W in both cases.

hour then gradually decreased for 10 hours. It indicates that O_2 concentration decreased with time. During the 1st hour O_2 concentration decreased from 20% to 5%, in the following 10 hours from 5% to almost 1%.

Figure 4.7 shows the variation of intensity of the spectrum in the UV region with

the variation of O_2 concentration in the "gas controlled tube" experiment whereas figure 4.8 shows the change of intensity in the UV region with operation time in the "closed tube" experiment.

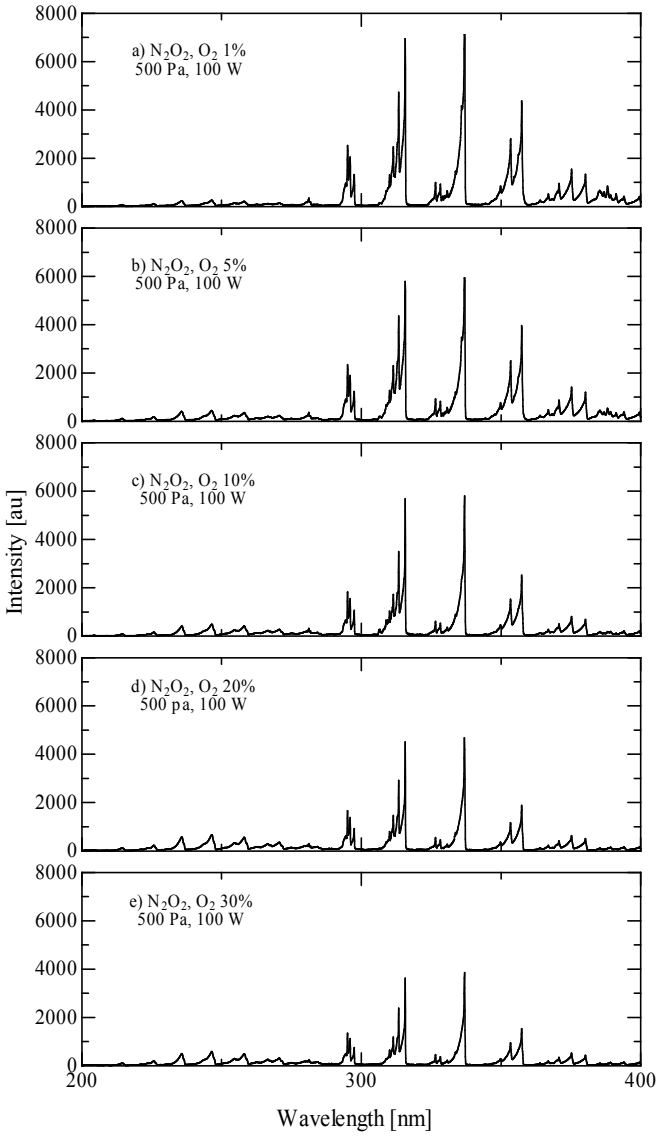

Fig. 4.7: Emission spectra from N_2/O_2 microwave discharge in the UV range at different O_2 concentration.

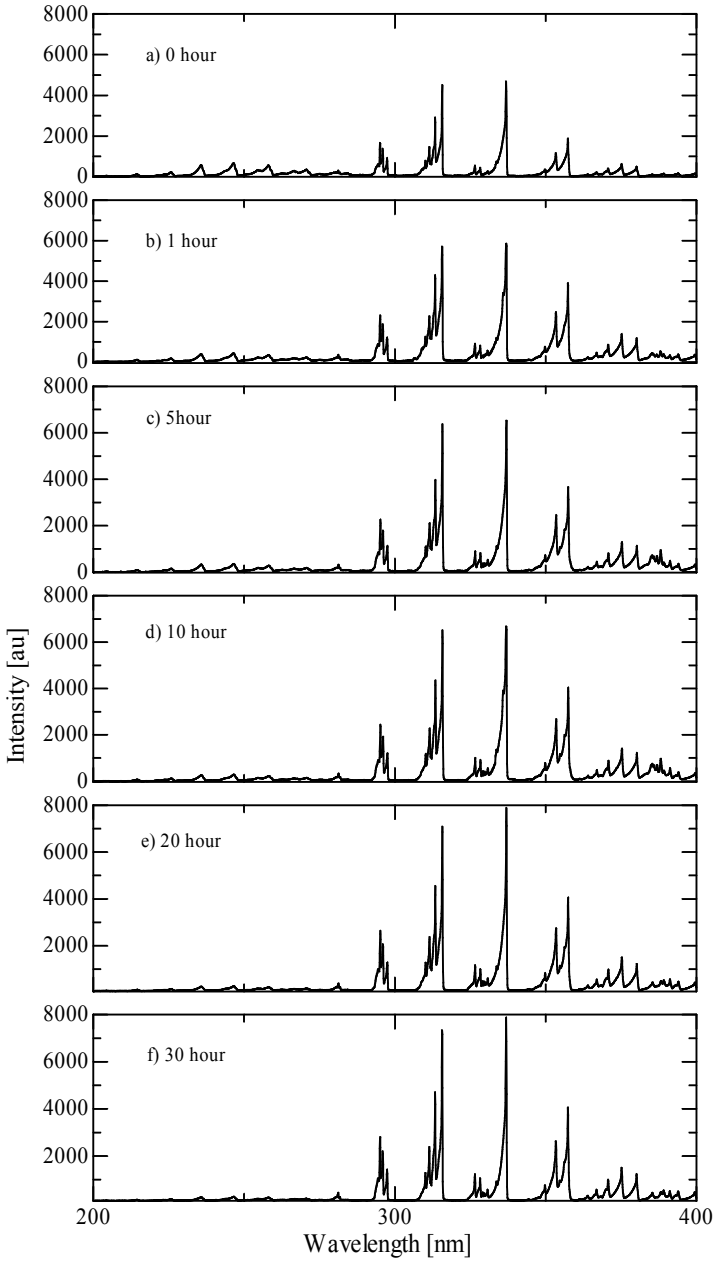

Fig. 4.8: Time dependent emission spectra from N_2/O_2 microwave discharge in "closed tube" experiment.

Figure 4.9(a) presents the effect of O_2 concentration on intensity ratio of 316nm N_2 (2^{nd} positive) peak to 247 nm NO peak from "gas controlled tube" and figure 4.9(b) presents the variation of intensity ratio of 316nm N_2 (2^{nd} positive) peak to 247 nm NO peak from "closed tube". It is observed from figure 4.9(a) that the intensity ratio decreases with increased O_2 concentration. The value of the ratio was almost 10 with 20% O_2 and it was almost 13 with 5% O_2. From figure 4.9(b), it can be found that the O_2 concentration decreases with time. Within 1 hour the intensity ratio decreased to almost 13 which

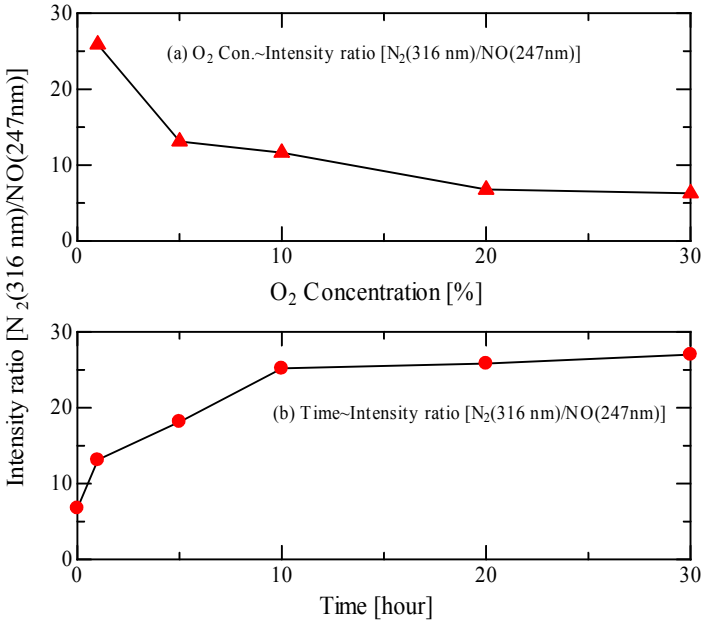

Fig. 4.9: Dependence of intensity ratio (316 nm peak /247 nm peak) with (a) O_2 concentration (pressure 500 Pa) and (b) Time.

means that within 1 hour the amount of O_2 decreased from 20% to about 5% and within

10 hours of operation O_2 concentration decreases to almost 1%. So from figures 4.6 and 4.9, we can conclude that O_2 concentration in the closed tube decreased with time.

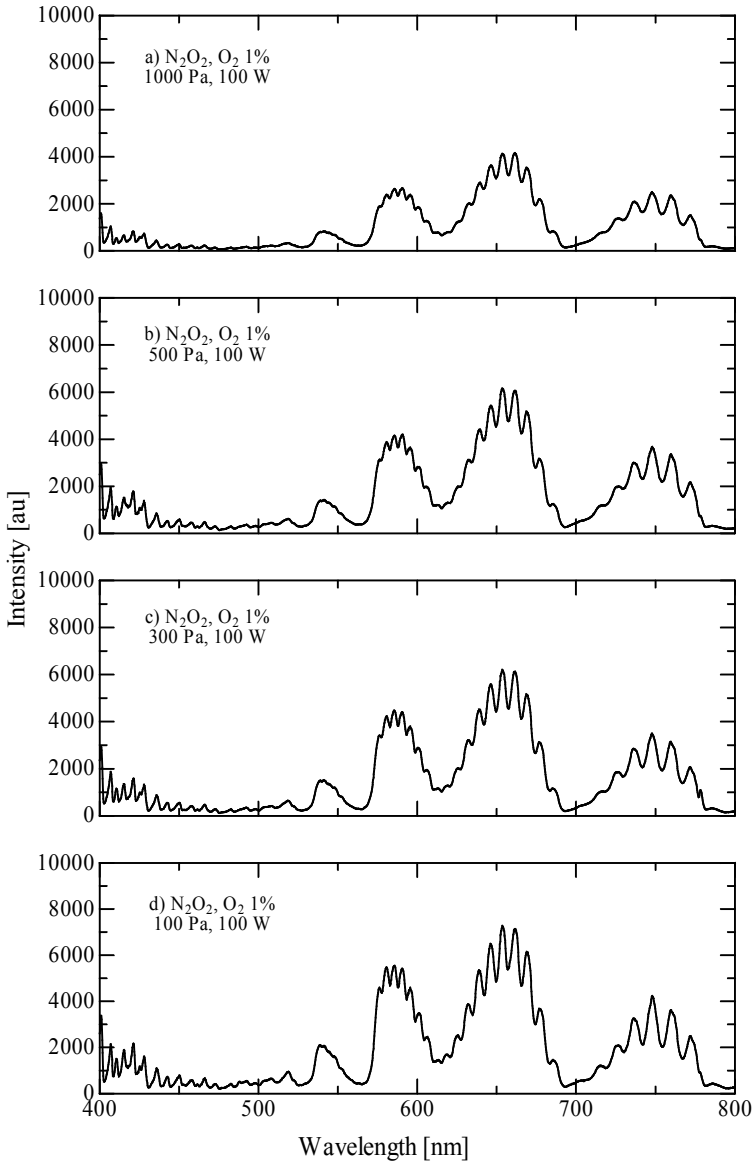

Fig. 4.10: Emission spectra from N_2/O_2 microwave discharge in the visible range at different pressure.

The dependence of the spectra in the visible region on the total pressure in the "gas

controlled tube" is shown in figure 4.10. The dependence of intensity ratio (750nm peak from 1st positive of N_2 to 540nm peak from 1st positive of N_2) on O_2 concentration and total pressure is shown in figures 4.11(a) and (b), respectively. From figure 4.11(a) it is found that the intensity ratio did not vary but remained almost same at different O_2

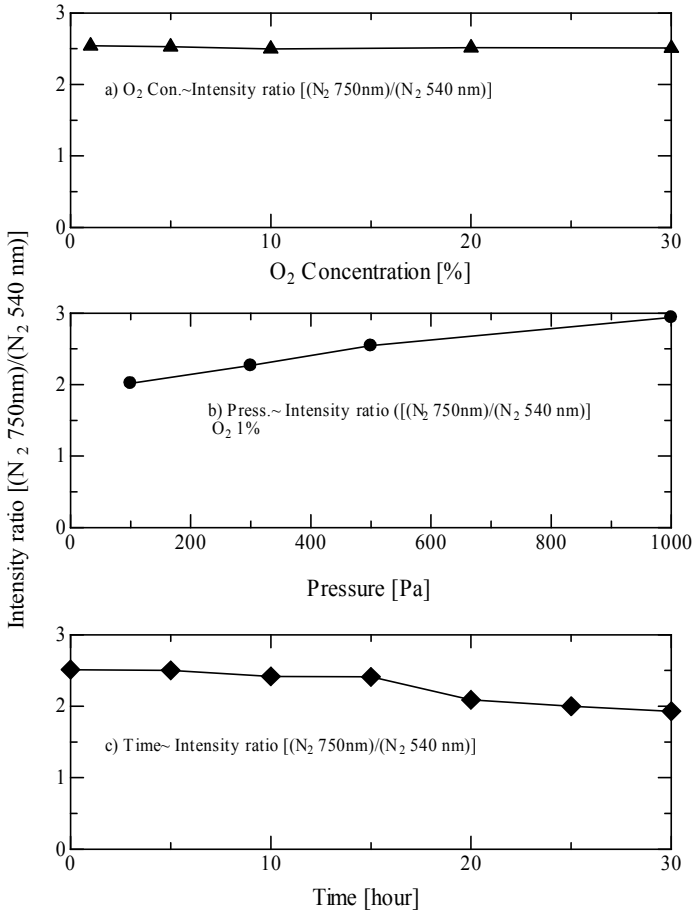

Fig. 4.11: Variation of intensity ratio (750 nm peak/540 nm peak) with (a) O_2 concentration (pressure 500 Pa), (b) Pressure (1% O_2 con.) and (c) Time.

concentration under same total pressure. On the other hand, figure 4.11(b) indicates that

the intensity ratio varied with total pressure at the same O_2 concentration. With the increase of pressure, the ratio also increased. The possible reason of the increase of the intensity ratio with pressure is that the two peaks have different upper energy states. The 750nm N_2 peak has lower energy state whereas the 540 nm N_2 peak has higher energy state. The electron temperature T_e increases with the decrease of pressure mostly due to increase of electron mean free path but T_e is not seriously affected by oxygen addition. Figure 4.11(c) shows the variation of intensity ratio with operation time of the closed tube. It is seen from this figure that, the ratio decreased with time and reached below 2 after 30 hours of operation. It can be estimated that pressure dropped below 100 Pa after 30 hours of operation and then the discharge stopped. In the "gas controlled tube", the minimum pressure was 100 Pa to sustain the plasma.

4.3 Conclusions

The N_2 /O_2 discharge emits UV light in the 210 nm to 300 nm region from NO molecules as the products in the plasma. The intensity of NO peaks decreased with time due to the decrease O_2 concentration inside the closed tube with operation time. Within 1 hour of operation, O_2 concentration decreased from 20% to 5% and in the following 10 hours O_2 concentration reached to almost 1%. The pressure of N_2 also decreased with time and after several 10 hours of operation the pressure dropped to a level which is not enough to sustain the plasma.

References

[1] R. W. B. Pears and A. G. Gaydon, Identification of Molecular Spectra, Chapman and Hall Ltd., London (1984)

Chapter 5

Estimation of effective germicidal UV power density emitted from N_2 /O_2 microwave plasma

In this chapter, the measurement technique and the comparison of the of the intensity of the emitted radiation in the UV region from the N_2/O_2 gas mixture microwave excited discharge and from low pressure commercial Hg lamp (MITSUBIHI/ OSRAM GL10) are discussed. UV light ranges from 200 to 400 nm however the whole range does not have germicidal effect. Only the radiation emitted between 210 and 315 nm has germicidal effect. The germicidal efficiency of the radiation emitted at different wavelength within this range is also not same. The potential germicidal efficiency coefficients at different wavelengths are different having the maximum at 260 nm. The estimation and comparison of the UV power density and effective germicidal power density emitted from N_2/O_2 gas mixture discharge and from low pressure commercial Hg lamp are also discussed in this chapter.

5.1 Experimental method

The schematic diagram of the experimental set-up for N_2/O_2 gas mixture microwave discharge is shown in Fig. 5.1. A one side closed quartz tube with 500 mm length, 15 mm outer diameter and 13 mm inner diameter was used for discharge. The tube was inserted into a discharge applicator with dimensions of 260 mm length, 100 mm width and 30 mm height. The open side of the quartz tube was connected to a gas supplying line for evacuating by using a oil rotary pump and for filling with different

concentration of N_2 and O_2 gas (both N_2 and O_2 were 99.99995% pure) at various pressure. The same magnetron power source which was used in the previous experiments was used in the experiment. After filling the discharge tube with gases,

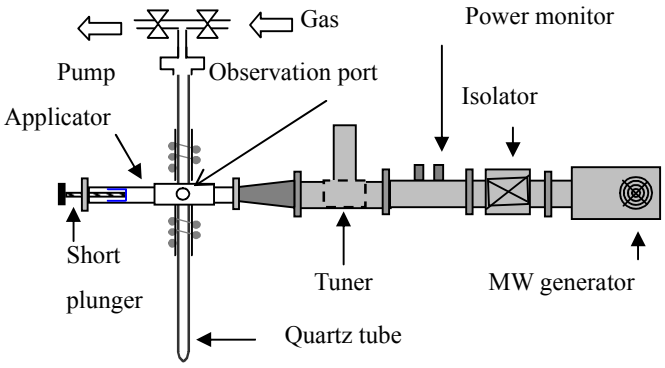

Fig. 5.1: Schematic diagram of the experimental set-up for N_2/O_2 discharge

microwave power of 100 W was supplied to the applicator and discharge was produced with the help of Tesla coil. Reflected power was adjusted to 0 W by using the tuner.

Optical emission spectroscopy was carried out using 2 sets of fiber coupled spectrometer, for UV (HR4000) and for visible light (USB4000) through a observation port consisting of a metal tube with 10 mm inner diameter and 40 mm length on the side wall of the microwave applicator. The optical fiber was set at the end of the port which was 10 cm away from the center of the discharge tube. The spectrometers with optical fibers were calibrated with standard Xe lamp (L7810-02, Hamamatsu Photonics, K.K) to confirm the absolute power.

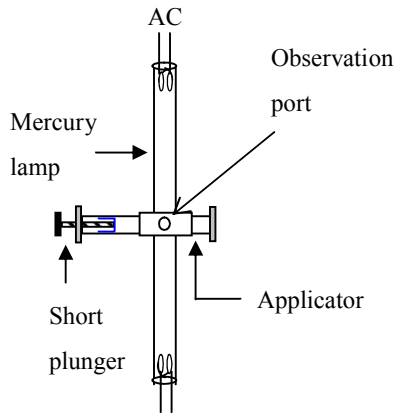

Fig. 5.2: Experimental set-up for power density measurement from mercury lamp

The UV power from a commercial low pressure mercury lamp (Mitsubishi/Osram GL10) was measured for comparison. The mercury lamp was operated by AC 100V (60 Hz) using a conventional lighting circuit. The measurement was carried out in the same configuration as in the case of N_2/O_2 microwave discharge. As shown in Fig. 5.2 the mercury lamp was inserted into the applicator for measuring the absolute power density.

5.2 Estimation of power density

5.2.1 Estimation of total UV power density

The emitted UV power density from N_2/O_2 microwave discharge was evaluated using the following equation

$$I = \sum \left[I(\lambda) \times \Delta\lambda \right], \text{ ---------- 5.1}$$

where

I = emitted power density in 200- 400 nm wavelength range (μW /cm^2)

$I(\lambda)$ = emitted power density at particular wavelength within a wavelength width $\Delta\lambda$ ($\mu W/cm^2$-nm)

$\Delta\lambda$ = wavelength width (nm).

$I(\lambda)$ is obtained from the measured spectra

$\Delta\lambda$ is obtained from the interval of wavelength of the spectra measured by spectrometer.

5.2.2 Estimation of power density in the germicidal region

Although UV light ranges from 200 to 400 nm, the whole range does not have germicidal effect. Only the range between 210 and 315 nm has germicidal effect. The energetic UV radiation in this region destroys microorganisms by killing or altering the structure of the DNA of the microorganisms [1]. The emitted power density in the germicidal region was estimated using the following equation

$$I = \sum [I(\lambda) \times \Delta\lambda \ ], \text{ ---------- 5.2}$$

where

I = emitted power density in the 210- 315 nm range ($\mu W /cm^2$)

$I(\lambda)$ = emitted power density at particular wavelength within a wavelength width $\Delta\lambda$ ($\mu W/cm^2$-nm)

$\Delta\lambda$ = wavelength width (nm).

$I(\lambda)$ is obtained from the measured spectra

$\Delta\lambda$ is obtained from the interval of wavelength of the spectra measured by spectrometer.

5.2.3 Estimation of effective germicidal power density

The germicidal efficiency of the emitted radiation at different wavelength is also not same over the whole germicidal region (210 to 315 nm). Numerical value for the potential germicidal efficiency coefficients at different wavelengths is different having the maximum at 260 nm. Numerical value for the potential germicidal efficiency coefficients at different wavelengths is listed in table 5.1 [2]. The effective germicidal power density was calculated ted using the following equation [2]

$I = \sum [I(\lambda) \times S(\lambda) \times \Delta\lambda\ ]$, ---------- 5.3

where

I = effective germicidal power density in the 210 to 315 nm range (μ W/ cm^2),

$I(\lambda)$ = emitted power density at particular wavelength within a wavelength width $\Delta\lambda$ (μW/cm^2-nm)

$S(\lambda)$ = germicidal efficiency coefficient of wavelength width $\Delta\lambda$ and

$\Delta\lambda$ = wavelength width (nm).

$I(\lambda)$ is obtained from the measured spectra

$\Delta\lambda$ is obtained from the interval of wavelength of the spectra measured by spectrometer.

$S(\lambda)$ was obtained from data published by Meulemans [3] which is given in table 5.1.

Table 5.1: Numerical value for the potential germicidal efficiency coefficients at different wavelengths

Wavelength	Efficiency Coefficient S(λ)

210	0.02
215	0.06
220	0.12
225	0.18
230	0.26
235	0.36
240	0.47
245	0.61
250	0.75
255	0.88
260	0.97
265	1.00
270	0.93
275	0.83
280	0.72
285	0.58
290	0.45
295	0.31
300	0.18
305	0.10
310	0.05
315	0

5.3 Results and discussion

Figure 5.3(a), shows the UV emission spectra from N_2/O_2 discharge at 20% O_2 concentration and 500 Pa total pressure. The peaks at 214, 225, 236 and 246 nm are from NO $\gamma(A^2\sum^+ - X^2\Pi)$ system, which is degraded to the shorter wavelength [4]. The emission spectrum from a commercial low pressure Hg lamp (Mitsubishi/Osram GL10) is shown in figure 5.3(b). The spectrum was measured with same measurement configuration as that of N_2/O_2 microwave discharge. Single peak at 254 nm was

observed in the 210 to 315 nm region.

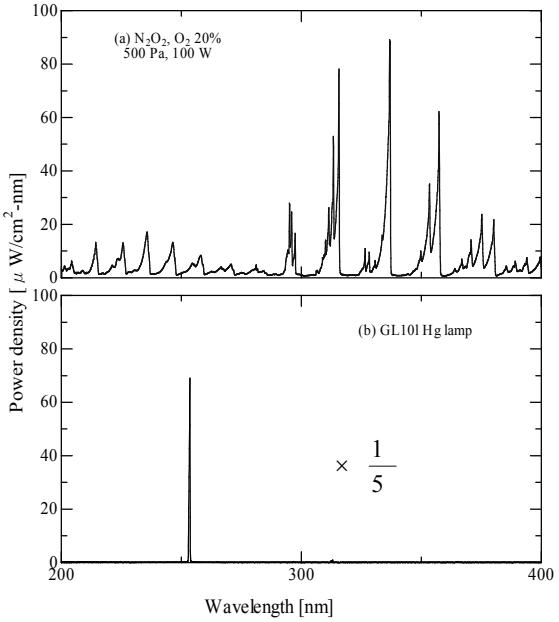

Fig. 5.3: Emission spectra in the UV range from (a) N_2 + 20% O_2 and (b): Emission spectra from commercial low pressure Hg lamp

The emitted power density in the UV region was calculated using equation 5.1. In the case of N_2/O_2 discharge, the UV (200- 400 nm) power density was 1100μW/cm^2. On the other hand, the UV (200- 400 nm) power density was 180μW/cm^2 from Hg lamp.

Figure 5.4(a), shows the spectra in the germicidal region from N_2/O_2 discharge at 20% O_2 concentration and 500 Pa total pressure. The spectra in the germicidal region emitted from a commercial low pressure mercury lamp are shown in figure 5.4(b). The emitted power density in the germicidal region was calculated using equation 5.2. The emitted power density in the germicidal region was 470 μW/cm^2 from N_2/O_2 discharge

whereas emitted power density in the germicidal region was 170 μW/cm^2 from Hg lamp.

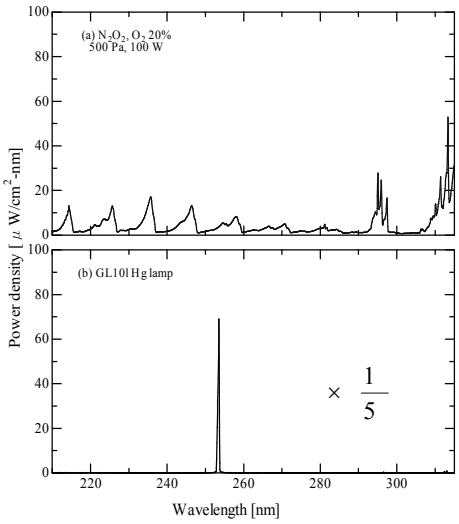

Fig. 5.4. Emission spectra in the germicidal region from (a) N_2/O_2 discharge and (b) a commercial low pressure mercury lamp.

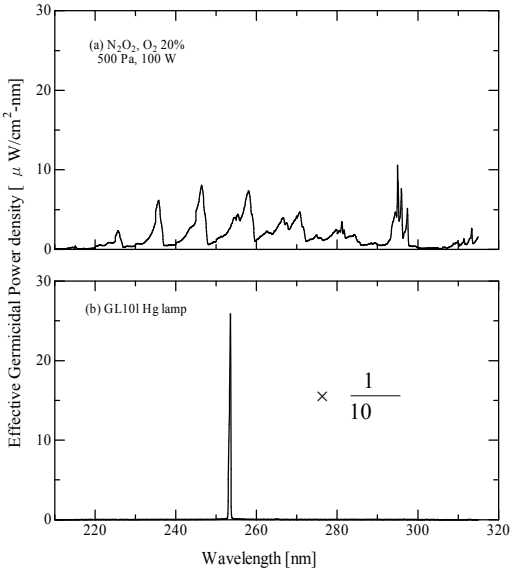

Fig. 5.5: Effective germicidal power density from (a) from N_2 /O_2 gas mixture discharge and (b) from commercial mercury lamp.

Figures 5.5(a) and (b) show the emission spectra from N_2 /O_2 gas mixture (20% O_2) at 500 Pa and from commercial mercury lamp. The density of the effective germicidal power was estimated using equation 5.3. The effective germicidal power density was 170 μW/cm^2 from N_2/O_2 discharge and whereas effective germicidal power density was 120 μW/cm^2 from GL10 lamp.

The findings of the above study are summarized in table 5.2.

Table 5.2: The findings of the study

Items	Hg lamp	N_2/O_2 discharge
UV (200-400 nm) density	180 μW/cm^2	1100 μW/cm^2
UV (210-315 nm) density	170 μW/cm^2	470 μW/cm^2
Effective germicidal power density	120 μW/cm^2	170 μW/cm^2
Most effective peak	254 nm	247 nm
Input power	10 W	100 W

5.4 Summary

N_2 /O_2 discharge emits intensive UV light in the 200 nm to 400 nm region. The maximum effective germicidal power density from N_2/O_2 discharge was obtained at total pressure 500 Pa, and at 80% N_2 and 20% O_2 concentration. The UV (200 -400 nm) power density was 1100 μW/cm^2 from N_2/O_2 discharge and was 180 μW/cm^2 from GL10 lamp. Power density in the germicidal range (210 nm t0 315 nm) was 470

$\mu W/cm^2$ from N_2/O_2 discharge and was 170 $\mu W/cm^2$ from GL10 lamp whereas the effective germicidal power density was 170 $\mu W/cm^2$ from N_2/O_2 discharge and was 120 $\mu W/cm^2$ from GL10 lamp.

In case of Hg lamp, 95% of the UV light is emitted in the germicidal region and 65% of the total UV light is effective in germicidal action. On the other hand, in case of N_2/O_2 discharge 45% of the UV light is emitted in the germicidal range and only 15% of it is effective in germicidal action.

References

[1] A. I. Al-Shamma: I. Pandidas and J. Lucas: J. Phys. D Appl. Phys. **34,** 2775 (2001).

[2] W. J. Massachelein, Ultraviolet light in Water and Wastewater Sanitation, Lewis, New York (2002).

[3] C. C. E. Meulemans, Proc. IOA Conference (1986).

]4] R. W. B. Pears and A. G. Gaydon, Identification of Molecular Spectra, Chapman and Hall Ltd., London (1984).

Chapter 6

Conclusions

UV radiations have many applications in biological, physical and chemical processes; such as disinfection of drinking water, sterilization of medical equipments, photochemical synthesis and photo-enhanced chemical vapor deposition. Mercury which is used today as filling element in the UV light source is highly toxic and potentially carcinogenic. Environmental groups worldwide are calling for limits on the use of mercury in electrical and electronic equipment. So the replacement of mercury in conventional UV lamps by other components is highly desirable for environmental reasons. Now it is high time to find out the alternative of mercury as a light source. As mentioned in chapter 1, molecular radiators can be new options as mercury free light source.

This research focuses on the study of the emission spectrum from N_2 /O_2 gas mixture discharge in the UV and visible range (from 200 – 800 nm) aiming to apply it as a mercury free UV light source which can be used for water purification. Discharge was produced in a quartz tube with 500 mm length and 15 mm outer diameter by applying microwave power. Microwave power was used for excitation of discharge to avoid degradation of molecular gases through chemical reactions with electrodes. The dependence of emission intensity emitted from microwave excited N_2 /O_2 discharge on gas composition and total pressure was examined. The effect of inert gases on the intensity of the emission was also investigated. Long time operation was also carried out to investigate the life time of the source. Power density in the UV and germicidal

region from N_2/O_2 discharge was measured in comparison with a low pressure commercial mercury lamp (GL10).. The effective germicidal power emitted from both mercury lamp and N_2/O_2 discharge was also estimated.

The main conclusions of this study are summarized as follows.

Chapter 2 Production UV emission from N_2/O_2 gas discharge

UV emission was produced from microwave excited N_2/O_2 gas mixture discharge in a cylindrical quartz tube. It was investigated that gas composition and the total pressure were critical factors influencing the intensity of UV emission emitted from NO molecules. The intensity of UV emission varied with gas composition and pressure, and was highest at 20% O_2 concentration and 500 Pa total pressure.

Chapter 3 Effect of rare gases and pulse operation

The effect of inert gases on the emission intensity was examined. He, Ne, Ar, Kr and Xe gases at different percentages of concentration was used in the experiment. It was observed that at low concentration below 5%, these gases have no effect on the emission intensity whereas the emission intensity in both the UV and visible ranges decreased as the rare gas concentration was increased. The gases only behave as buffer gases. Buffer gases caused collisions with the other co-existing molecules and decreases the emission intensity.

UV intensity in 200- 400 nm region does not vary with pulse width and pulse interval but depends on average power. The life time of NO molecules is shorter than 1 ms.

Chapter 4 Long time operation of N_2/O_2 discharge

The long time operation of microwave excited N_2/O_2 gas mixture discharge without refreshing the enclosed gas was performed. It was observed that the UV intensity emitted from NO molecules decreased with time due to the decrease of O_2 concentration inside the closed tube with operation time. Within 1 hour of operation, O_2 concentration decreased from 20% to 5% and in the following 10 hours O_2 concentration reached to almost 1%. The pressure of N_2 also decreased with time. After several 10 hours of operation the pressure of N_2 dropped to a level which was not enough to sustain the plasma.

Chapter 5 Estimation of UV power density

Power density in the UV (200- 400 nm) and germicidal (210- 315 nm) region emitted from the N_2/O_2 discharge and from low pressure commercial Hg lamp (MITSUBIHI/ OSRAM GL10) was measured and compared. The UV (200 -400 nm) power density was 1100 $\mu W/cm^2$ from N_2/O_2 discharge and was 180 $\mu W/cm^2$ from GL10 lamp. Power density in the germicidal range was 470 $\mu W/ cm^2$ from N_2/O_2 discharge on the other hand power density in the germicidal range was 170 $\mu W/ cm^2$ from GL10. The effective germicidal power density emitted from both N_2/O_2 discharge and mercury lamp was also estimated. The effective germicidal power density was 170 $\mu W/ cm^2$ from N_2/O_2 discharge whereas effective germicidal power density was 120 $\mu W/ cm^2$ from GL10 lamp. In case of Hg lamp, 95% of the UV light is emitted in the germicidal region and 65% of the total UV light is effective in germicidal action. On the other hand, in case of N_2/O_2 discharge, 45% of the UV light is emitted in the germicidal range and only 15% of it is effective in germicidal action.

As N_2/O_2 discharge produces effective germicidal power density of 120 μ W/ cm^2, this can be used for water purification purpose. However further research should be carried out to increase the efficiency and the life time of the source.